

Differences in Intrinsic Properties and Local Network Connectivity of Identified Layer 5 and Layer 6 Adult Mouse Auditory Corticothalamic Neurons Support a Dual Corticothalamic Projection Hypothesis

Daniel A. Llano^{1,2} and S. Murray Sherman²

¹Department of Neurology and ²Department of Neurobiology, University of Chicago, Chicago, IL 60637, USA

Intrinsic properties, morphology, and local network circuitry of identified layer 5 and layer 6 auditory corticothalamic neurons were compared. We injected fluorescent microspheres into the mouse auditory thalamus to prelabel corticothalamic neurons, then recorded and filled labeled layer 5 or layer 6 auditory cortical neurons in vitro. We observed low-threshold bursting in adult, but not juvenile, layer 5 corticothalamic neurons that was voltage and time dependent with nonlinear input-output properties, whereas adult layer 6 corticothalamic neurons demonstrated a regular spiking. Layer 5 corticothalamic neurons had larger somata, thicker apical dendrites and were more likely to have a layer 1 apical dendrite than layer 6 neurons. Using laser photostimulation, identified layer 5 corticothalamic neurons received excitatory input from a wide area of layers 2/3, 4, and 5 with widespread γ -aminobutyric acidergic input from layer 2/3 and lower layer 5, whereas layer 6 corticothalamic neurons from the same cortical column received circumscribed excitatory input and discrete patches of inhibition derived from layer 6 of adjacent columns. These data demonstrate that layer 5 and layer 6 corticothalamic neurons receive unique sets of inputs and process them in different manners, supporting the hypothesis that layer-specific corticothalamic projections play distinct roles in information processing.

Keywords: cortex, corticothalamic, laser, layer, thalamus

Introduction

Corticothalamic projections emanate from layers 5 and 6 and vastly outnumber the ascending sensory afferents in all sensory portions of the thalamus (Wilson et al. 1984; Van Horn et al. 2000; Jones 2002). Most previous physiological studies of these systems have relied on stimulation or inactivation of large groups of cortical neurons, without layer specificity. As a result, multiple theories surrounding the role of these descending inputs have been proposed (Castelo-Branco et al. 1998; Suga and Ma 2003; Sillito et al. 2006). We have described the presence of at least 2 distinct corticothalamic projection systems that differ in their layer of origin, their site of termination within the thalamus, and the characteristics of their thalamic terminals (for review, see Sherman and Guillery 2002). These projections are comprised of a feedforward system emanating from layer 5 that project via large, proximally situated synapses to higher order parts of the thalamus and a feedback system emanating from layer 6 that uses small terminals on distal thalamic dendrites (Wilson et al. 1984; Hoogland et al. 1987; Rouiller and Welker 1991; Deschênes et al. 1994; Ojima 1994; Rouiller and Durif 2004). These anatomical specializations in layer 5 and layer 6 corticothalamic projections manifest in distinct EPSP signatures. In the somatosensory system, layer 5 activation in vitro

produces large, all-or-none EPSPs in thalamic cells that show paired-pulse depression and activate ionotropic but not metabotropic glutamate receptors (“Driver” synapses, Reichova and Sherman 2004, Groh et al. 2008), whereas layer 6 activation produces small, graded and facilitating EPSPs that activate both ionotropic and metabotropic receptors (“Modulator” synapses, Reichova and Sherman 2004). In addition, visual and auditory layer 5 corticothalamic projections are organized in a non-reciprocal manner, such that their thalamic target regions project to areas of the cortex outside of their source of layer 5 innervation. In contrast, layer 6 corticothalamic–thalamocortical projection system is reciprocally organized (Van Horn and Sherman 2004; Llano and Sherman 2008). Based on these data, we have proposed that layer 5 corticothalamic neurons serve primarily a feedforward role, defining the receptive field properties of higher order thalamic neurons, whereas layer 6 neurons provide feedback information, modulating the excitability of thalamic neurons (Sherman 2007).

Lacking in this model, however, is a description of the intrinsic and local network processing that shapes the output of either layer 5 or layer 6 corticothalamic neurons (Sherman and Guillery 1998). Within layer 5 of the primary sensory cortices, there are at least 2 classes of projection neurons based on electrophysiological and anatomic criteria. “Intrinsic bursting” neurons are large pyramidal neurons with thick apical dendrites with an apical tuft extending into layer 1. In response to depolarizing pulses, these neurons fire a characteristic burst of action potentials (Connors et al. 1982; Chagnac-Amitai et al. 1990; Larkman and Mason 1990; Mason and Larkman 1990; Kasper et al. 1994; Schwindt et al. 1997; Hefti and Smith 2000). In the visual and somatosensory systems, intrinsic bursting cells project to the midbrain and brainstem (Wang and McCormick 1993; Kasper et al. 1994; Rumberger et al. 1998; Christophe et al. 2005). “Regular spiking” neurons are pyramidal as well but have smaller cell bodies and have thin apical dendrites that rarely extend into layer 1. In response to depolarizing pulses, these neurons fire a train of individual action potentials and show spike frequency adaptation (Connors et al. 1982; Chagnac-Amitai et al. 1990; Larkman and Mason 1990; Mason and Larkman 1990; Kasper et al. 1994; Hefti and Smith 2000) and tend to project to the contralateral hemisphere (Kasper et al. 1994; Christophe et al. 2005; Le Be et al. 2007; Ramos et al. 2008).

To our knowledge, only one other study has looked at the intrinsic electrical properties of layer 5 corticothalamic neurons. Hattox and Nelson (2007) studied layer 5 corticothalamic projections in the juvenile mouse somatosensory system and found that such cells share the morphological characteristics of intrinsic bursting cells but display regular spiking patterns. This same study did not find bursting in any

layer 5 neurons, irrespective of their postsynaptic targets. It has not been shown in any system whether “adult” layer 5 corticothalamic neurons are intrinsic bursting, regular spiking, or a mixture of types.

There has been comparatively little work investigating properties of either auditory layer 5 or layer 6 corticothalamic systems. Ojima et al. (1992) found that large pyramidal auditory cortical neurons, morphologically similar to intrinsic bursting neurons described above, in upper layer 5 projected to the diencephalon. In addition, this group analyzed the detailed structure of 4 layer 6 auditory corticothalamic neurons and found them to all have a pyramidal morphology, but of small somatic size, with short apical dendrites and minimal horizontal collaterals, which would be consistent with work in other systems (Zhang and Deschenes 1997). Other work in layer 6 of the cat demonstrated that corticothalamic neurons were pyramidal in morphology and had a wide range of diameters (Prieto and Winer 1999). To our knowledge, the physiological properties of either cell type have not been investigated.

The potential differences in morphological properties of layer 5 and layer 6 corticothalamic neurons would suggest that these neurons integrate local input differently. Several investigators have studied local synaptic input maps to layer 5 and layer 6 neurons using scanning photolysis of caged glutamate but have often found significant heterogeneity in these maps (Briggs and Callaway 2001, 2005; Schubert et al. 2001, 2006; Zarrinpar and Callaway 2006). None of these investigators have looked at input maps to identify corticothalamic neurons and therefore none have compared such maps between layer 5 and layer 6 neurons sharing a cortical column. In the current study, therefore, we examine the morphological and physiological properties of preidentified adult mouse auditory layer 5 and layer 6 corticothalamic neurons and compare the local synaptic input maps of layer 5 and layer 6 corticothalamic neurons residing in the same cortical column using scanning laser photolysis of caged glutamate.

Methods

General Preparation and Recording Methods

Adult (60 days) and juvenile (22–30 days) Balb/c mice of both sexes were used for this study. All surgical procedures were approved by the Institutional Animal Care and Use Committee at the University of Chicago, and animals were housed in animal care facilities approved by the American Association for Accreditation of Laboratory Animal Care. Every attempt was made to minimize the number of animals used and to reduce suffering at all stages of the study. Mice were anesthetized with ketamine hydrochloride (100 mg/kg) and xylazine (3 mg/kg) and placed in a stereotaxic apparatus. Aseptic conditions were maintained throughout the surgery. Response to toe pinch was monitored, and supplements of anesthesia were administered when needed. Injection targets in the thalamus were localized using stereotaxic coordinates (3.5 mm posterior to bregma, 1.5 mm lateral to midline, and 2.5 mm depth from dorsal surface). Micropipettes (tip diameter 10 μm) were filled with 50–75 nL of rhodamine-tagged polystyrene microspheres (Fluospheres, Invitrogen, Carlsbad, CA) and injected into the auditory thalamus or contralateral auditory cortex over a duration of 20–30 min using a nanoliter injector governed by a microsyringe pump controller (World Precision Instruments, Sarasota, FL). Most thalamic injection sites filled the dorsal division of the auditory thalamus with some spillover into the ventral and medial divisions. Because there is very little input from cortical layer 5 to the ventral division of the auditory thalamus (Llano and Sherman 2008), we assume that the majority of the labeled layer 5 cells project to the dorsal

and medial divisions of the auditory thalamus. Animals were allowed to survive for 24–72 h prior to sacrifice. Injection sites were verified during the recording experiment by observing these sites with fluorescence optics. Slices from injections with significant spillover outside the auditory thalamus or auditory cortex were eliminated.

To obtain slices, each animal was deeply anesthetized by intraperitoneal injection of pentobarbital (50 mg/kg), perfused with an ice-cold high-sucrose cutting solution (in mM: 206 sucrose, 10.0 MgCl_2 , 11.0 glucose, 1.25 NaH_2PO_4 , 26 NaHCO_3 , 0.5 CaCl_2 , 2.5 KCl, pH 7.4), and its brain was quickly removed. Coronal tissue slices (300 μm) were cut using a vibrating tissue slicer and transferred to a holding chamber containing oxygenated incubation artificial cerebrospinal fluid (ACSF) (in mM: 126 NaCl, 3.0 MgCl_2 , 10.0 glucose, 1.25 NaH_2PO_4 , 26 NaHCO_3 , 1.0 CaCl_2 , 2.5 KCl, pH 7.4) and incubated at 30 $^\circ\text{C}$ for 1 h prior to recording. For experiments involving mapping of synaptic inputs to corticothalamic cells using laser uncaging of glutamate, the N-methyl-D-aspartic acid (NMDA)-blocker MK-801 (Sigma, St Louis, MO) at 6 μM was added to the incubation medium (see below for rationale).

Whole-cell recordings were performed using a visualized slice setup outfitted with infrared-differential interference contrast (IR-DIC) optics and performed at 30–34 $^\circ\text{C}$. During recordings, tissue was bathed in recording ACSF (in mM: 126 NaCl, 1.0 MgCl_2 , 10.0 glucose, 1.25 NaH_2PO_4 , 26 NaHCO_3 , 3.0 CaCl_2 , 2.5 KCl, pH 7.4). Recording pipettes were pulled from borosilicate glass capillary tubes and had tip resistances of 2–4 M Ω when filled with solution, which contained (in mM: 117 K-gluconate, 13 KCl, 1.0 MgCl_2 , 0.07 CaCl_2 , 0.1 ethyleneglycol-bis(2-aminoethylether)-*N,N,N,N'*-tetra acetic acid, 10.0 4-(2-hydroxyethyl)-1-piperazineethanesulfonic acid, 2.0 Na-ATP, 0.4 Na-GTP, and 0.5% biocytin, pH 7.3). Corticothalamic or corticocortical neurons were identified by fluorescence optics (Zeiss filter set #15: Excitation filter BP 546/12, Emission filter LP 590, Dichroic FT 580). For illustration of typical thalamic injection site and pattern of cortical labeling, see Figure 1. In this figure, layer 5 and layer 6 labels are seen in the primary auditory cortex, consistent with previous findings (Llano and Sherman 2008). We used the Multiclamp 700B amplifier (Axon Instruments, Sunnyvale, CA) and pClamp software (Molecular Devices) for data acquisition, which was done at 20 kHz. We recorded from retrogradely labeled neurons in the primary auditory cortex in a whole-cell configuration. For generation of synaptic input maps, most recordings were in A1 near the A1/A2 border, where there is a high concentration of labeled layer 5 and layer 6 corticothalamic neurons. The A1/A2 border was distinguishable based on the increased density of myelination of A1 relative to A2 (Meltzer and Ryugo 2006). Here, recordings of these neurons were performed in the same 100 μm wide cortical column. The access resistance of the cells was constantly monitored throughout the recordings, and recordings were limited to neurons with a stable access of <30 M Ω throughout the experiment. We injected constant-amplitude depolarizing current pulses into neurons to determine their firing mode (bursting vs. regular spiking). Bursting neurons were defined by the presence of 3 or more spikes occurring in rapid succession, with a decrement in amplitude with each succeeding spike, all of which riding a crest of slow depolarization (Connors et al. 1982). In our experience, which is consistent that described by other investigators (Connors et al. 1982; Kasper et al. 1994; Hefti and Smith 2000), the distinction between intrinsic bursting and regular spiking is not subtle, and methods beyond visual inspection have not been necessary to delineate between the 2 firing modes. Occasionally, we have seen failure of the third spike during a burst in a neuron demonstrating clear bursting earlier in an experiment, and in these cases only, doublets are considered bursts.

Physiological Analysis

We used Clampfit (Molecular Devices) for all analyses. In most cases, we used 400-ms long current pulses in 50 pA steps to characterize neuronal response properties. Spontaneous activity was extremely rare, so firing threshold was defined as the lowest amplitude depolarizing pulse that elicited an action potential. To compare our data with previous work on identified corticothalamic and corticocortical neurons in the juvenile somatosensory system (Hattox and Nelson 2007), we studied the slow adaptation properties, fast

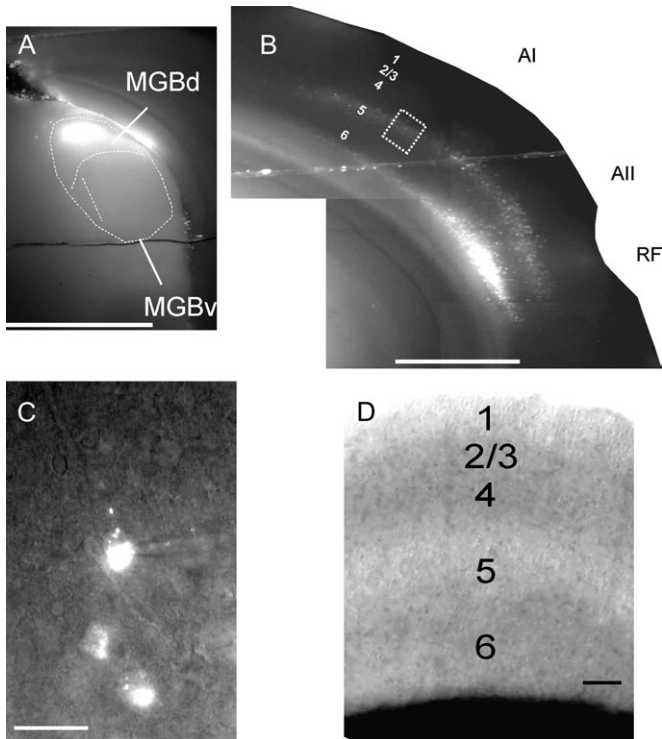


Figure 1. Fluorescent (Zeiss filter set #15; Excitation filter BP 546/12, Emission filter LP 590, Dichroic FT 580) photos, taken as monochrome and of a slice while in the recording apparatus. (A) The $\times 5$ photograph of typical injection site in the medial geniculate body. MGBd = dorsal division of the MGB. MGBv = ventral division of the medial geniculate body. (B) Retrograde cortical labeling in the same slice. Note that the MGBd injection produces retrogradely labeled neurons in layers 5 and 6 of the auditory cortex, with a predominance of layer 5 label in the primary auditory cortex (AI) and both layers 5 and 6 of the secondary auditory cortex (AII). RF = rhinal fissure. Scale bar for (A, B) = 1 mm. (C) The $\times 40$ view of labeled cells from dotted box in (B). A patch pipette is shown patched onto the top cell. Scale bar = 25 μm . (D) The $\times 10$ IR-DIC photograph of the primary auditory cortex while in the recording chamber to illustrate the lamination patterns used to designate individual layers in this study. Scale bar = 100 μm .

afterhyperpolarizations (fAHP) and depolarizing afterpotentials (DAP) for our cells. The adaptation index was defined as

$$\text{Adaptation Index} = \frac{\text{ISI}(\text{between last 2 spikes}) - \text{ISI}(\text{between spikes 3 and 4})}{\text{ISI}(\text{between last 2 spikes})}$$

where ISI = interspike interval, for a 400-ms current pulse at 200 pA above spiking threshold. Adaptation indices closer to 1.0 indicate a larger degree of adaptation. The fAHP has been shown to be a point of differentiation between different classes of layer 5 neurons (Hattox and Nelson 2007) and to be important in determining the adaptation properties of pyramidal neurons (Gu et al. 2007). The fAHP was defined as the difference between the voltage just prior to the rising fast phase of the action potential and the minimum voltage occurring within 2 ms after the action potential. The DAP was defined as the difference between the voltage minimum immediately after an action potential and the voltage maximum occurring in the 10-ms period after this minimum (for an example, see Fig. 4). Previous work has shown that intrinsic bursting and the DAP are both calcium-dependent (Friedman and Gutnick 1989; Mason and Larkman 1990; Friedman et al. 1992), and we hypothesize that the DAP may be present in nonburst spikes from cells that also demonstrate intrinsic bursting. The output metric for input-output curves was generated by counting the number of spikes in a 25-ms window after the response onset at each stimulus amplitude. For paired-pulse paradigms, 10-ms depolarizing pulses near burst threshold were used and were presented at interpulse intervals of 500,

250, 125, 62.5, 31.25, and 16 ms. Hyperpolarization-activated cation currents (I_h) were measured in response to hyperpolarizing pulses of -200 pA. Voltage changes were converted into currents to allow comparison of layer 5 and layer 6 neurons, which have different input resistances (see Results) and therefore generate different voltage deflections to similar values of I_h . The difference between the negative most voltage within the first 100 ms of the hyperpolarizing pulse and the plateau voltage during the 200–400 ms was converted into an inward current using the input resistance of the cell ($V_{\text{peak}}/200$ pA):

$$I_h = \frac{|(V_{\text{peak}} - V_{\text{plateau}})|}{(V_{\text{peak}}/200 \text{ pA})}$$

The membrane time constant (τ_{membrane}) was computed by fitting a single exponential function to the first 100 ms of the voltage change induced by injection of 50 pA negative current. Curve fitting was done using Clampfit (Molecular Devices).

Photostimulation

We used our previously described methods for photostimulation (Lam and Sherman 2005). Data acquisition and photostimulation were controlled by a program written in Matlab (MathWorks, Natick, MA) developed in the laboratory of Karel Svoboda. Nitroindolyl-caged glutamate (Sigma-RBI, Natick, MA) was added to recirculating ACSF to a concentration of 0.39 mM during recording. Focal photolysis of the caged glutamate was accomplished by a pulsed UV laser (355 nm wavelength, frequency-tripled Nd:YVO₄, 100-kHz pulse repetition rate; DPSS Laser, San Jose, CA). The laser beam was directed into the side port on top of a Zeiss microscope (Axioskop 2 FS plus) using UV-enhanced aluminum mirrors (Thorlabs, Newton, NJ) and a pair of mirror galvanometers (Cambridge Technology, Cambridge, MA) and then focused onto the brain slice using a low-magnification objective (5×0.1 , Zeiss). Angles of the galvanometers were computer-controlled. The optics were designed to generate a nearly cylindrical beam in the slice so as to keep the mapping 2 dimensional (Shepherd et al. 2003). The Q-switch of the laser and a shutter (LS3-ZM2; Vincent Associate, Rochester, NY) controlled the timing of the laser pulse for stimulation. A thin microscope coverslip in the laser path reflected a small portion of the laser onto a photodiode. The current output from this photodiode was amplified, acquired by the computer, and used to monitor the laser intensity during the experiment. Photodiode output was calibrated to laser power at the back focal plane of the objective when we set up the optical equipment.

The standard stimulation pattern for mapping the input to corticothalamic neurons consisted of positions arranged in a 16×16 array, with 75 μm between adjacent rows and columns. We used 75 μm spacing (rather than 50 μm , used by others; Schubert et al. 2006; Zarrinpar and Callaway 2006) in order to cast a wide enough net to capture a maximum number of local inputs in a 16×16 array. To avoid receptor desensitization, local caged-glutamate depletion, and excitotoxicity, stimulation of these positions was arranged in a sequence that maximized the distance between consecutive trials. The light stimulus was 2 ms long, which consisted of 200 laser pulses. The time interval between photostimuli was 1 s. The laser power used (measured at the back focal plane of the objective) ranged from 8 to 40 mW. The transmittance of the objective is 60% at 355 nm wavelength. In our experience, we have not seen any change of the recording quality during experiments that suggested damage from phototoxicity.

Neurons were held in voltage clamp at -40 mV to assess both excitatory and inhibitory inputs. This value was chosen based on the estimated reversal potential of chloride in our experiments of -55 mV, yielding an adequate driving force to observe outward currents. Three synaptic input maps were generated for each neuron. The first map was generated in normal ACSF. We refer to the map generated using normal ACSF as the “total” input map, reflecting direct activation of the recorded neuron by the uncaging of glutamate as well as synaptic activation. The second map was generated in ACSF with low Ca^{2+} and high Mg^{2+} (0.2 mM CaCl_2 , 4.0 mM MgCl_2 , all other ACSF parameters were the same) to block synaptic transmission. We refer to the map generated under high-magnesium, low-calcium conditions as the “direct” input map, reflecting

only direct activation of the recorded neuron by the uncaging of glutamate. The third map was generated after the washout of the low Ca^{2+} /high Mg^{2+} solution and the washing in of normal ACSF. The currents generated during low Ca^{2+} /high Mg^{2+} map was subtracted from the normal ACSF map to generate a final synaptic input map. The washout map was not used in the subtraction algorithm. Because NMDA channels are likely to be unblocked at -40 mV with normal ACSF but blocked with high-magnesium ACSF, we blocked NMDA channels under all conditions by incorporating the NMDA-blocker MK-801 ($6 \mu\text{M}$) in our incubation medium. For some neurons where inhibition was found, we incorporated blockers of γ -aminobutyric acid (GABA)_A receptors (SR 95531 at $1 \mu\text{M}$, Tocris) to determine the neurotransmitter and receptor responsible for the inhibition.

One potential concern regarding the interpretation of activation sites found during photostimulation runs is the potential for distal dendritic activation. Dendritic activation could lead to misattribution of the layer of origin of a particular synaptic connection. This concern has been addressed by Shepherd et al. (2003), who demonstrated in loose-seal recording mode under "synaptic blockade" that spiking was only generated when cells were stimulated over the cell body or proximal dendrites. Another possible concern is the potential for polysynaptic activation by the laser. This issue has been addressed by Katz and Dalva (1994) who did not find suprathreshold activation at cortical sites outside of the stimulation zone. Shepherd et al. (2003) report similar results and have estimated the degree of synaptic driving to account for less than 1% of cortical synaptic responses.

Responses were analyzed using programs written in Matlab. At all stimulation sites, a 100-ms window immediately following the stimulus pulse was used for analysis. For each analysis window, a baseline value, taken as the mean of the preceding 100 ms, was subtracted. Each 100-ms analysis window obtained in low Ca^{2+} /high Mg^{2+} ACSF was subtracted from the same window obtained in normal ACSF. The response was then parsed into negative values (inward currents) and positive values (outward currents), which are assumed to be excitatory or inhibitory, respectively. The parsing of currents into inward and outward directions generated 2 maps: one reflecting excitatory input to the recorded neuron and the other reflecting inhibitory input. The total amount of inward or outward charge transfer was displayed at each point on the map. In our experience, spontaneous excitatory post-synaptic potential and inhibitory post-synaptic potential are uncommon, and the responses to photostimulation can be easily detected by their short latency and the presence of similar responses in adjacent stimulation locations.

For quantitative comparison of input maps to layer 5 corticothalamic neurons versus layer 6 corticothalamic neurons, we sequentially recorded from pairs of neurons in a single column and compared both the number of sites where either excitation or inhibition could be elicited and the overall width of contiguous sites providing either excitation or inhibition. For any given site on our 16×16 array, we determined whether there was a significant difference between the current generated in normal ACSF versus low Ca^{2+} /high Mg^{2+} ACSF by comparing the means of the current generated under the 2 conditions using a *t*-test (using $P < 0.0002$, which is a Bonferroni-corrected value). Both the number of sites with significant activation and the width of activation were compared between layer 5 and layer 6 corticothalamic neurons.

Correlation of photostimulation site with a cortical layer was made by overlaying the 16×16 grid of stimulation points with a high-contrast IR-DIC brightfield photograph of the $\times 5$ magnification (see Fig. 1D). We made no attempt to distinguish sublayers within layer 5 or 6 because the potential demarcations within these layers were neither obvious nor consistent. We did not find robust differences between layers 2/3 and 4 using low-power IR-DIC. These differences are apparent under high power, and in our experience with Nissl staining in the primary auditory cortex, layers 2/3 and 4 occupy equal proportions of the highly cellular dark band shown in Figure 1D. We therefore assigned the upper half of this band to layer 2/3 and the lower half to layer 4.

Histology

Cells were filled with biocytin by diffusion. After recording, slices were fixed in 4% paraformaldehyde in 0.01M phosphate-buffered saline (PBS) for at least 24 h. Slices were then exposed to 0.5% hydrogen peroxide

for 30 min to quench endogenous peroxidases, washed 3 times in PBS, and then immersed in 0.3% Triton-X (Sigma) to enhance membrane permeability. Sections were then incubated for 4 h at room temperature with peroxidase-based ABC reagent (Vectastain Elite ABC-Peroxidase Kit, Vector, Burlingame, CA) and washed in PBS, followed by 2 washes in Tris-buffered saline at pH 8.0. Visualization of label was done by using a cobalt-intensified, diaminobenzidine reaction (Sigma-Fast tablets). Whole sections were mounted in 100% glycerol and were visualized using a Leica DM5000B microscope. All photographs were taken with Leica $\times 10$ NPLAN, NA 0.25 objective, and Retiga 2000R camera. Image processing was done with Qcapture Pro software. Because whole sections ($300 \mu\text{m}$) were used, a series of photographs were taken at approximately 500 nm steps through each neuron, and then imported as a stack into ImageJ (<http://rsb.info.nih.gov/ij/>), where a minimum intensity projection image was created. Cross-sectional areas were computed by creating a polygon around the perimeter of each cell body and measuring the area using ImageJ. Radial dendritic lengths were measured by measuring the linear distance from the cell body, radially, to the most distal dendrite. Dendritic thickness was measured $10 \mu\text{m}$ distal to the transition point between the cell body and the dendrite and was done under immersion using a Leica NPLAN $\times 100/1.25$ objective. Morphological analysis in this study was restricted to somatic and dendritic features because the focus of the current study is on the local input circuitry of layer 5 versus layer 6 corticothalamic neurons.

Although an attempt was made to label all adult neurons that were recorded, the general yield of recovered cells in this study is low (ca. 15–20%). This is likely related to the large amount of positive pressure needed to clear the dense neuropil present in the adult brain, which created tight, difficult to dislodge, seals. Only a limited number of cells were recovered in juvenile samples because these cells were obtained as part of a pilot study.

Statistical Analysis

The major hypothesis of this study is that layer 5 and layer 6 corticothalamic neurons have different roles and therefore have different physiological, anatomical, and/or local network properties. As such, the primary analysis in all cases is between adult layers 5 and layer 6 corticothalamic neurons to limit the influence of multiple comparisons leading to potential type I error. For comparisons of multiple physiological parameters between cell classes, we have conservatively corrected for multiple comparisons using a Bonferroni correction.

Comparisons with less than 20 observations in a group were done with nonparametric tests (Kruskal-Wallis for >2 groups and Mann-Whitney for 2 groups). For comparisons of greater than 20 observations, we assessed normality of the distributions using a χ^2 goodness-of-fit test to a hypothetical normal distribution having the same mean and standard deviation. All differences having $P > 0.05$ were considered to have a normal distribution and were analyzed using a student's *t*-test. Kruskal-Wallis or Mann-Whitney was used for the remainder. Comparison of distributions of inputs from different cortical layers was done with χ^2 test on a 5×2 matrix. All measurements are given as mean \pm standard deviation.

Results

Summary of Database

We recorded and analyzed 47 adult and 32 juvenile layer 5 corticothalamic neurons and 24 adult layer 6 corticothalamic neurons and 36 adult layer 5 corticocallosoal neurons. For morphological analysis, we recovered and analyzed 12 adult corticothalamic neurons and 9 adult layer 6 corticothalamic neurons. As mentioned above, the majority of the analysis is focused on the comparison between layer 5 and layer 6 corticothalamic neurons in adult animals. Comparison to layer 5 corticocallosoal or to juvenile neuronal properties will be discussed when comparing our data to those of other groups or

where a notable difference has been observed between groups (e.g., in bursting behavior).

Comparison of Intrinsic Membrane and Firing Properties

We compared layer 5 and layer 6 neurons across 9 physiological parameters and therefore considered P values of less than 0.0056 significant. Comparison of passive properties between layer 5 and layer 6 corticothalamic neurons revealed a lower input resistance of layer 5 corticothalamic neurons compared with layer 6 corticothalamic neurons (125 ± 41 M Ω vs. 216 ± 93 M Ω , $P < 0.001$, t -test), which likely corresponds to the larger size of the neurons in layer 5 (see Morphological Differences between Groups). Layer 5 and layer 6 neurons did not differ in their resting membrane potentials (Layer 5 corticothalamic = -60.6 ± 6.1 mV; Layer 6 corticothalamic = -63.9 ± 7.0 mV, $P = 0.06$, t -test) or membrane time constants (Layer 5 corticothalamic = 17.0 ± 6.5 ms; Layer 6 corticothalamic = 14.6 ± 5.6 ms, $P = 0.134$, t -test).

The majority of the adult layer 5 corticothalamic neurons (32/47 or 68.1%) demonstrated bursting at spike threshold in response to depolarizing current pulses (herein referred to as low-threshold bursting). An example of low-threshold bursting behavior is seen in Figure 2A. In response to a 400-ms positive

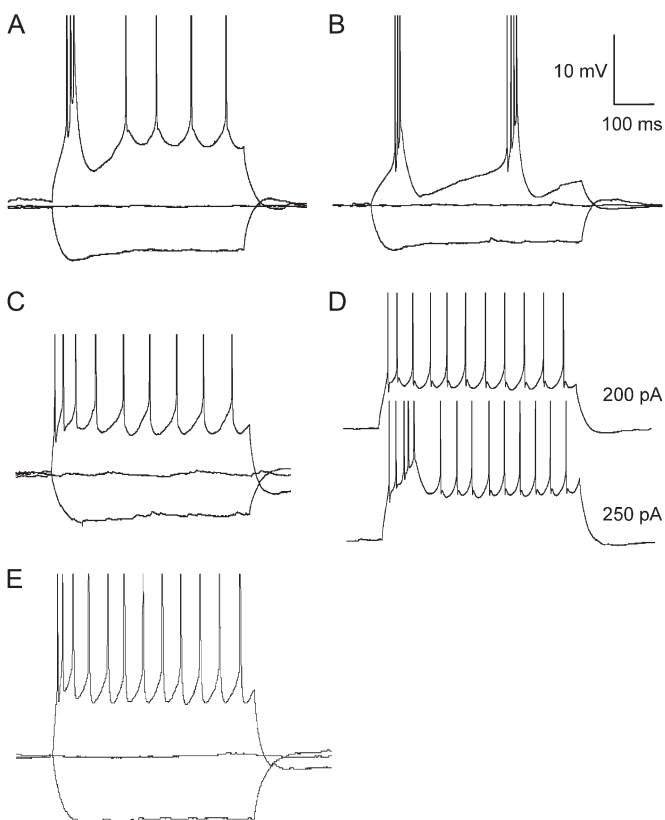


Figure 2. Examples of firing modes observed in corticothalamic neurons. (A) Layer 5 low-threshold bursting neuron, demonstrating a burst of fast action potentials riding a slow depolarizing wave at stimulus onset. (B) A small number (7/34) of layer 5 low-threshold bursting cells showed repetitive bursting at low threshold. (C) Regular spiking layer 5 corticothalamic neuron. In this case, the neuron fires a train of individual action potentials in response to a 200 pA current step and then fires a burst of action potentials in response to a 250 pA current step. (D) Example of a high-threshold bursting neuron. In this case, the neuron fires a train of individual action potentials in response to a 200 pA current step and then fires a burst of action potentials in response to a 250 pA current step. (E) Example of a layer 6 corticothalamic neuron. This neuron fires a train of individual action potentials in response to a depolarizing pulse. Action potential heights are truncated for clarity.

current injection, this neuron demonstrated a slowly rising depolarization crowned by 3 action potentials. Thereafter, this neuron discharged a series of individual action potentials. A minority of low-threshold bursting neurons (7/30) demonstrated rhythmic bursting (Fig. 2B). Six of the 7 rhythmic bursting neurons converted to burst-tonic modes as stimulus amplitude exceeded 400 pA. Of the 15 neurons that were not low-threshold bursting neurons, 13 showed a regular spiking pattern (Fig. 2C). That is, they fired trains of individual action potentials in response to depolarizing current pulses. The 2 remaining neurons had regular spiking patterns at spike threshold and demonstrated a burst at the onset of higher amplitude depolarizing pulses (Fig. 2D). Consistent with the description and nomenclature of Schwandt et al. (1997), we refer to these cells as high-threshold bursting neurons. In both cases, bursting was seen at 200 pA above firing threshold. No bursting was observed in any layer 6 corticothalamic neurons, and all such neurons demonstrated regular spiking profiles (Fig. 2E). To determine if bursting is a general property of layer 5 cells, we examined the firing properties of 36 layer 5 corticocollateral neurons and found that no cells demonstrated bursting. The 32/36 cells had regular spiking profiles and 4/36 demonstrated a single spike at onset at all suprathreshold pulse amplitudes.

Hyperpolarization elicited a prominent inward current, I_h , in layer 5 corticothalamic neurons (41.7 ± 21.2 pA at 200 pA negative current injection), observable in the traces in Figure 2A,B. I_h was significantly greater in layer 5 corticothalamic neurons than that seen in layer 6 corticothalamic neurons (14.9 ± 15.3 pA, $P < 0.001$, t -test; see Fig. 2E). The difference seen in values for I_h likely represents an underestimate of the density of hyperpolarization-activated cation channels because the more depolarized resting potentials and lower input resistances of layer 5 cells produced smaller hyperpolarizations in response to 200 pA of injected negative current (hyperpolarization peak for layer 5 corticothalamic cells = -82.6 ± 8.5 vs. -95.1 ± 9.1 mV for layer 6 cells, $P < 0.001$, t -test). Given the reversal potential of I_h of approximately -17 to -40 mV (McCormick and Pape 1990; Maccaferri et al. 1993), this represents a decreased driving force for I_h in layer 5 corticothalamic neurons.

Because thalamic neuronal responses to high frequency stimulation of layer 5 and layer 6 differ substantially (Reichova and Sherman 2004), we assessed corticothalamic neurons' ability to sustain high firing rates by using an adaptation index (see Methods). Adaptation indices were only computed for regular spiking neurons because bursting produces adaptation index values that are highly dependent on the specific intervals that are chosen. The adaptation index was larger for layer 6 corticothalamic cells (0.35 ± 0.13) than layer 5 corticothalamic cells (0.18 ± 0.14 , $P < 0.002$, Mann-Whitney). Despite the prominence of adaptation in layer 6 corticothalamic cells, the final interspike intervals were not significantly different when comparing layer 5 versus layer 6 corticothalamic neurons (48.1 ± 12.2 ms for layer 5 vs. 43.7 ± 10.8 ms for layer 6, $P = 0.284$, Mann-Whitney). These data suggest that although layer 6 neurons display greater adaptation than their layer 5 counterparts, they maintain a higher average firing rate throughout the 400-ms stimulus.

Layer 5 and layer 6 corticothalamic neurons also differed in their afterpotentials. Layer 5 corticothalamic neurons had a more prominent DAP than layer 6 neurons (2.2 ± 1.0 vs. 0.4 ± 1.0 mV, $P < 0.001$, t -test), whereas layer 6 neurons had a more prominent fAHP (8.8 ± 4.7 vs. 4.0 ± 3.7 mV, $P < 0.001$, t -test). See Figure 3

for examples and Table 1 for a summary of comparisons between layer 5 and layer 6 corticothalamic neurons.

Morphological Differences between Groups

We found that layer 5 and layer 6 corticothalamic neurons could be distinguished based on their somatic size as well as apical dendritic morphology, thickness, and length. Layer 5 corticothalamic cells had a larger somatic cross-sectional area than layer 6 corticothalamic neurons (193 ± 53 vs. $100 \pm 34 \mu\text{m}^2$, $P < 0.001$, Mann-Whitney), which is consistent with the greater input resistance of layer 6 neurons, described above. We also found that 10/12 adult layer 5 corticothalamic neurons that were recovered had a thick apical dendrite extending with a tuft into layer 1 of the cortex (for an example, see Fig. 4A). The remaining 2 neurons were pyramidal neurons with a thick apical dendrite that extended into layer 4 and had no apical tuft. The 8/10 neurons that had an apical tuft demonstrated

low-threshold bursting and the 2 neurons without an apical tuft also demonstrated low-threshold bursting. Layer 6 neurons were also pyramidal in morphology but had thinner apical dendrites that extended for shorter distances, ranging from remaining within layer 6 to extending into layer 4 (see Fig. 4B). Quantitatively, we found that the radial dendritic length and thickness of layer 5 corticothalamic neurons were greater than for layer 6 corticothalamic neurons (Length: 600 ± 233 vs. $198 \pm 176 \mu\text{m}$, $P < 0.001$, Mann-Whitney. Thickness: 3.7 ± 1.4 vs. $1.4 \pm 0.4 \mu\text{m}$, $P < 0.001$, Mann-Whitney). These data are summarized in Table 1.

Investigations of Bursting Behavior

We compared a subset of relevant physiological parameters (resting potential, input resistance, membrane time constant, I_h , afterhyperpolarizing potential, and DAP) between bursting and nonbursting layer 5 corticothalamic cells to determine if these

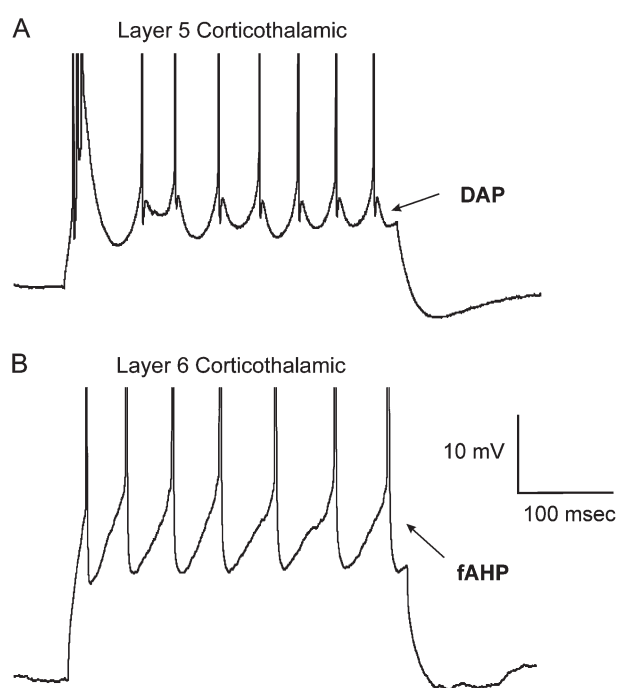


Figure 3. Examples of postspike potentials from (A) a layer 5 corticothalamic neuron and (B) a layer 6 corticothalamic neuron illustrating the prominent DAP in the layer 5 neuron and the prominent fAHP in the layer 6 neuron. Only spikes after the initial burst in bursting neurons were used to measure both the fAHP and the DAP. Action potential heights are truncated for clarity.

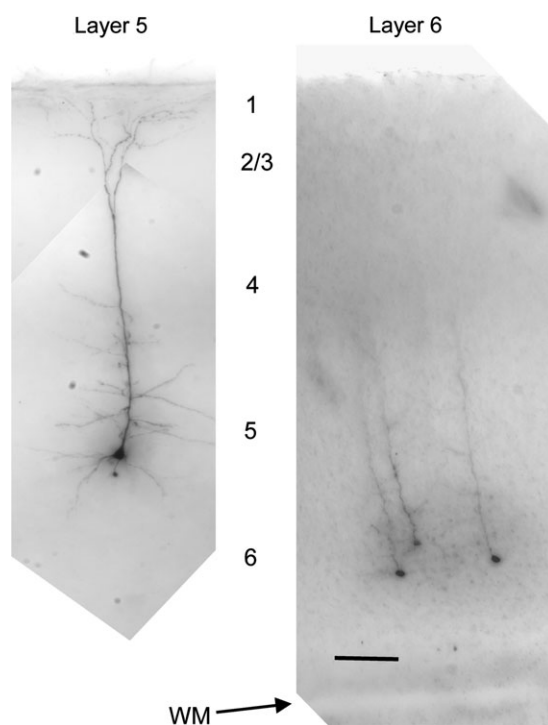


Figure 4. Examples of morphology of layer 5 and layer 6 corticothalamic neurons. (A) Minimum intensity projection of a typical biocytin-filled layer 5 corticothalamic neuron. (B) Minimum intensity projection of 3 biocytin-filled layer 6 corticothalamic neurons. These neurons have thin apical dendrite that do not extend above layer 4. Scale bar = $100 \mu\text{m}$.

Table 1

Summary of comparisons between layer 5 and layer 6 corticothalamic neurons

	Layer 5 corticothalamic ($n = 47$)	Layer 6 corticothalamic ($n = 24$)	P value
Ratio of cells with bursting	34/47	0/24	<0.00001
Input resistance ($M\Omega$)	125 ± 41	216 ± 93	<0.001
Resting potential (mV)	60.6 ± 6.1	63.9 ± 7.0	0.06
τ_{membrane} (ms)	17.0 ± 16.5	14.6 ± 5.6	0.134
I_h (pA)	41.7 ± 22.2	14.9 ± 15.3	<0.001
Adaptation index	0.18 ± 0.14 ($n = 13$)	0.35 ± 0.13 ($n = 21$)	0.002
Final interspike interval (ms)	48.1 ± 12.2 ($n = 13$)	43.7 ± 10.8 ($n = 21$)	0.284
DAP (mV)	2.1 ± 2.5	0.4 ± 1.0	<0.001
AHP (mV)	4.0 ± 3.7	8.8 ± 4.7	<0.001
Cells with layer 1 apical dendrite	10/12	0/9	<0.001
Somatic area (μm^2)	193 ± 53 ($n = 12$)	100 ± 34 ($n = 9$)	<0.001
Apical dendritic radial length (μm)	600 ± 233	233 ± 176	<0.001
Apical dendritic thickness (μm)	3.7 ± 1.4	1.4 ± 0.4	<0.001

comprise 2 classes of layer 5 corticothalamic neuron. We found that there were no differences in any of these parameters with the exception of a nonsignificant trend for lower input resistance in bursting cells (119 ± 38 vs. 144 ± 44 M Ω , $P = 0.073$, Mann-Whitney). Morphologically, as mentioned above, bursting was observed in cells with and without an apical dendritic tuft. Too few regular spiking cells ($n = 2$) were recovered for statistical analysis of morphological parameters in these 2 groups.

The input-output properties of low-threshold bursting and regular spiking adult layer 5 corticothalamic neurons were compared. Near-threshold, bursting tended to show all-or-none behavior, typically producing a burst of 3 action potentials at threshold (Fig. 5A, left). In contrast, regular spiking cells showed a single action potential at threshold and gradually

increased the number of action potentials as the amount of current injected was increased (Fig. 5B, right). These differences are summarized in Figure 5B. We examined the input-output relationship of low-threshold bursting versus regular spiking layer 5 corticothalamic neurons over the first 25 ms of a neuron's response. This window was chosen because it approximates 1.5X the membrane time constant of pyramidal neurons (mean τ_{membrane} for layer 5 corticothalamic neurons in current study = 17.0 ± 6.5 ms). We found that regular spiking neurons displayed a gradual increase in spike output as injected current increased, demonstrating fairly linear behavior. In contrast, low-threshold bursting neurons had very steep input-output functions at threshold, demonstrating nonlinear, all-or-none behavior.

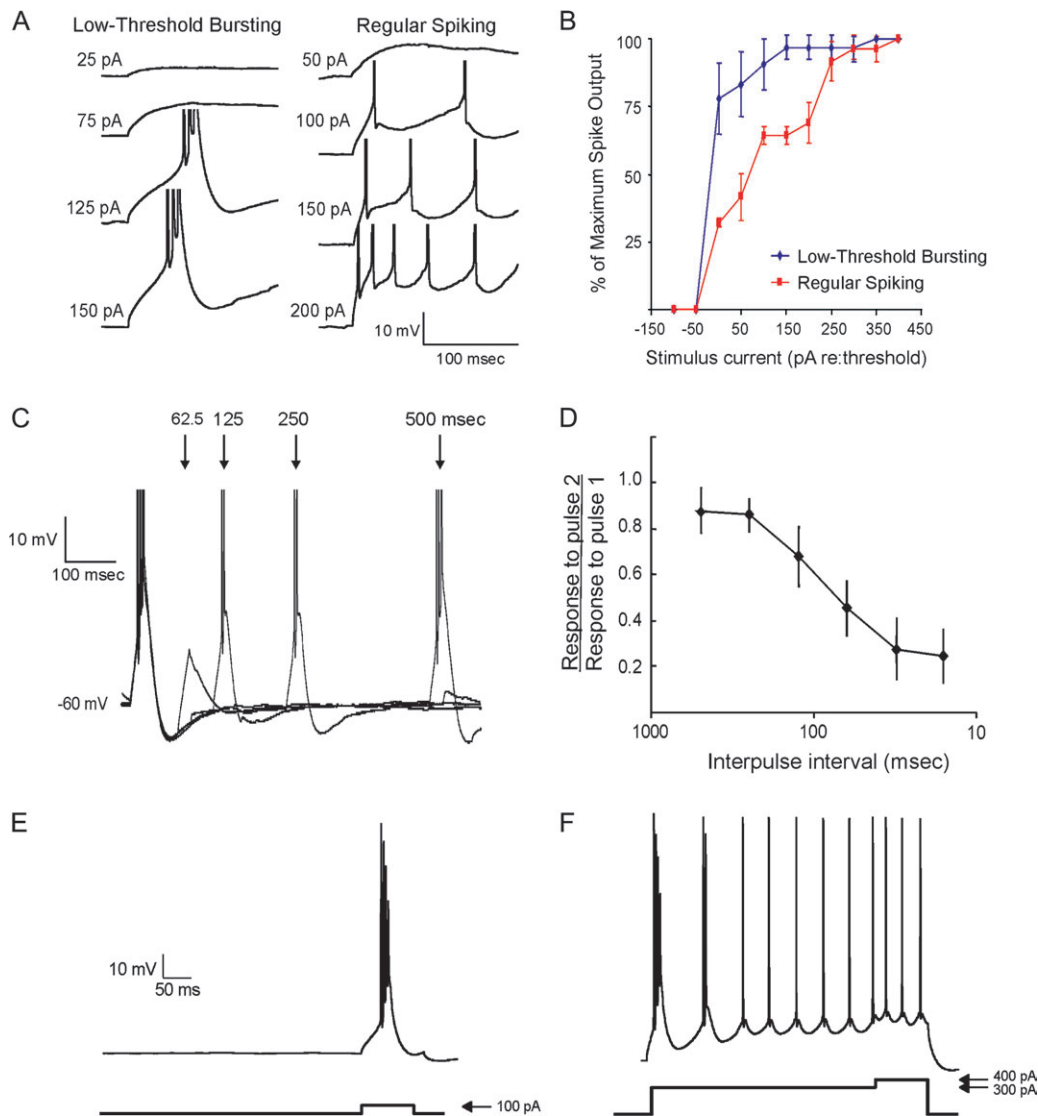


Figure 5. Characteristics of bursting: input-output functions, time dependence, and voltage-dependence. (A) Left: example of a low-threshold bursting neuron's response to increasing depolarizing pulse amplitude. Right: example of a regular spiking neuron's response to increasing depolarizing pulse amplitude. Both neurons are layer 5 corticothalamic neurons. Spikes are truncated in height for clarity. (B) Mean input-output functions for low-threshold bursting (blue) and regular spiking (red) layer 5 corticothalamic neurons. Error bars represent the standard deviation (SD). The y -axis shows number of spikes expressed as a percentage of the maximum number of spikes fired in a 25-ms window after response onset. (C) Response of low-threshold bursting neurons to paired-pulse stimulation. Shown in an overlay of 4 traces of a single neuron in response to interstimulus intervals of 62.5, 125, 250, and 500 ms. Action potential heights are truncated for clarity. (D) Interpulse interval versus average of the ratio of spike output in response to the second pulse to spike output in response to the first pulse. Error bars represent the SD at each point. (E) Response of a low-threshold bursting neuron to a depolarizing prepulse. This neuron responded to a 100 pA depolarizing pulse with a typical low-threshold burst. (F) After this cell is depolarized by about 10 mV by a 300 pA depolarizing pulse and recharged with 100 pA positive current pulse, this cell fired only individual spikes rather than a burst.

The time dependence of bursting was investigated using a paired-pulse paradigm. Figure 5C shows the typical response of a low-threshold bursting neuron. This neuron fired identical 3-spike bursts at interstimulus intervals of 500 ms, but as the ISI decreased to 250 and 125 ms, the neuron fired 2-spike bursts, and failed to burst at 62.5 ms. We tested the effects of shortening the interstimulus intervals on 8 low-threshold bursting neurons. We found that the average interstimulus interval that caused a drop in average spike output to 50% of baseline level was 89.6 ± 57 ms, which corresponds to a pulse rate of 11.2 pulses per second. The average interstimulus interval versus paired-pulse output ratio is shown in Figure 5D. Long interburst intervals were also seen in rhythmic bursting cells (e.g., Fig. 2B). In this population, the mean interburst interval at 50 pA above threshold was 213 ± 58 ms (range 119 to 299 ms), which translates into a bursting rate of 4.7 bursts/s. Assuming that bursts are encoded postsynaptically as unitary events (Lisman 1997), this rate of bursting is unlikely to cause significant adaptation in layer 5 corticothalamic synapses, which tend to show adaptation at stimulation rates greater than 10 Hz (Reichova and Sherman 2004).

The voltage dependence of low-threshold bursting was investigated in 7 neurons. In these cells, a prepolarizing pulse was applied prior to a test pulse known to evoke a low-threshold burst. An example of a typical response is shown in Figure 5E,F. This cell normally responded to a 100 pA current pulse with a burst of action potentials (Fig. 5E). When given a 400-ms pulse that depolarized the cell by about 10 mV, the 100 pA pulse (added on to the 300 pA depolarizing pulse) was unable to elicit a burst (Fig. 5F). Note that when not prepolarized, bursting in this cell was seen at all amplitudes greater than 50 pA. The elimination of bursting by prepolarization was seen in 6/7 cells tested. The average amount of depolarization used was 15.4 ± 5.1 mV, though the amount of depolarization needed to eliminate low-threshold bursting was not systematically investigated. In all cases, tonic depolarization led to a regular spiking after an initial burst during the prepulse.

Age and DAP Dependence of Bursting

In contrast to adult layer 5 corticothalamic neurons, we did not observe bursting in any juvenile layer 5 corticothalamic neurons. We compared several physiological parameters between adult and juvenile layer 5 corticothalamic neurons (see Table 2) and found that adult layer 5 cells had a significantly lower input resistance, lower membrane time constant, and DAP.

Of the 4 cell types and ages examined in this study (adult layer 5 corticothalamic, juvenile layer 5 corticothalamic, adult layer 5 corticocollal, and adult layer 6 corticocollal), only adult layer 5 corticothalamic neurons demonstrated bursting behavior.

Table 2
Summary of comparisons between juvenile and adult layer 5 corticothalamic neurons

	Juvenile layer 5 corticothalamic (n = 35)	Adult layer 5 corticothalamic (n = 47)	P value
Ratio of cells with bursting	0/32	34/47	<0.001
Input resistance (M Ω)	176 ± 87	125 ± 41	0.006
Resting potential (mV)	63.3 ± 7.3	60.6 ± 6.1	0.115
τ_{membrane} (ms)	28.4 ± 12.8	17.0 ± 16.5	0.001
I_h (pA)	44.8 ± 22.7	41.7 ± 22.2	0.554
DAP (mW)	0.84 ± 1.1	2.1 ± 2.4	0.003
AHP (mW)	2.7 ± 2.9	4.0 ± 3.7	0.082

Given the purported calcium dependence of both the DAP and bursting (Friedman and Gutnick 1989; Mason and Larkman 1990; Friedman et al. 1992), we compared the amplitude of the DAP across all these cell types and found a significant difference across the groups, with layer 5 corticothalamic cells having the highest value (Fig. 6; $P < 0.01$, Kruskal-Wallis).

Determination of Local Input Maps to Layer 5 and Layer 6 Corticothalamic Neurons

We recorded from 7 sequentially recorded pairs of identified layer 5 and layer 6 corticothalamic neurons from the same cortical column and used laser scanning photostimulation of caged glutamate to determine the pattern of inputs to each cell type.

As described in the Methods, each point on the array represents the total (direct and synaptic) current input to a neuron, and therefore, a second map was generated in low- Ca^{2+} /high- Mg^{2+} ACSF, and this latter map was subtracted from the first map to obtain a map of only synaptic inputs. Figure 7 demonstrates the subtraction algorithm. Figure 7A demonstrates a series of current traces elicited by photostimulation at various sites around the recorded cell, whereas the tissue is bathed in normal ACSF. Figure 7B demonstrates tracings from the same cell, elicited by stimulation of the same sites shown in Figure 7A, but while bathed in low- Ca^{2+} /high- Mg^{2+} ACSF (synaptic blockade). Figure 7C,D illustrates current traces from 2 sites—one from layer 2/3 (Fig. 7C) and another from lower layer 5 (Fig. 7D), demonstrating synaptic excitation and inhibition, respectively. Note in Figure 7C that the total and direct current traces overlap in time, compromising any time window method of separating direct versus synaptic activation. After subtraction, each trace is rectified to keep either the positive (outward) or negative (inward) current values, and therefore, 2 maps were generated, one for inward (presumed excitatory) and one for outward (presumed inhibitory) charge transfer. An example of a layer 5 and coregistered layer 6 recording is shown in Figure 8. Figure 8A,B illustrates current traces for the 256 tested sites for a layer 5 and layer 6 cell, both held at -40 mV. Figure 8C,D shows pseudocolor maps of the amount of inward, and Figure 8E,F shows outward charge transfer induced by photostimulation at the various stimulus sites, respectively. As shown, this pair of corticothalamic neurons in the same cortical column receive different patterns

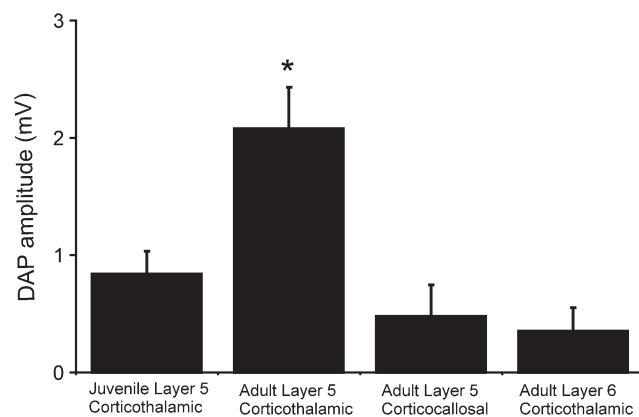


Figure 6. Bar graph illustrating differences in the magnitude of the DAP in 4 groups of neurons investigated in this study. Error bars represent standard error. * $P < 0.01$, Kruskal-Wallis.

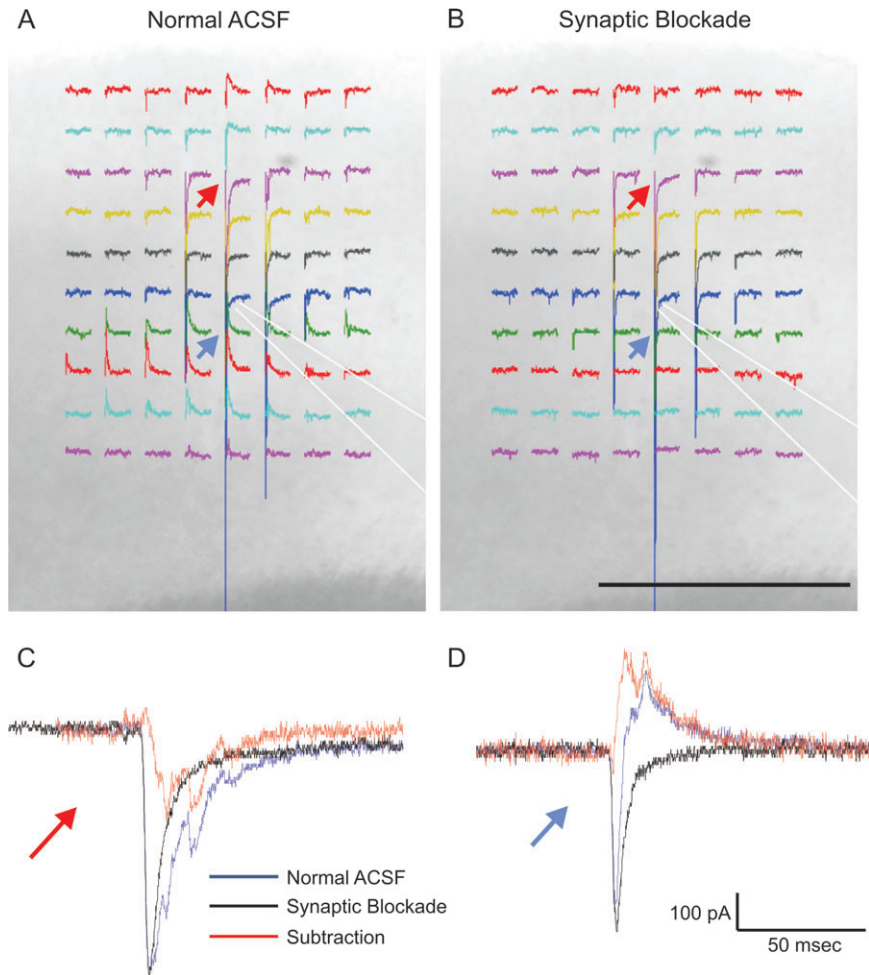


Figure 7. Illustration of synaptic blockade subtraction algorithm. (A) Photograph taken at $\times 5$ of cortical slice with overlay of current traces at several photostimulation sites obtained in normal ACSF. Recording electrode location is outlined with white dotted lines. Recorded cell is held in voltage clamp at -40 mV. (B) Same stimulation sites with tissue bathed in 0 mM CaCl_2 and 4 mM MgCl_2 . Scale bar = 500 μm . (C) Overlay of current traces at site in layer 2/3 with red arrow. Blue trace obtained in normal ACSF, black trace obtained in low calcium/high magnesium. Red trace is the difference of the normal ACSF and the low calcium/high magnesium traces. (D) Same description as (C) but for site in layer 5 with blue arrow.

of input, such that the layer 5 neurons receive both excitatory and inhibitory input from a larger number and wider breadth of stimulus sites than does the layer 6 corticothalamic neuron. Specifically, the layer 5 neuron receives excitatory input from layers 2/3, 4, and 5 and inhibitory input from layer 2/3 and lower layer 5, whereas the layer 6 neuron receives excitatory input locally from layer 6 and lower layer 5, with a minimum of inhibitory input.

We found that layer 5 corticothalamic neurons received a greater amount of inward synaptic current, expressed as total charge transfer and summed across all 256 stimulus sites, than layer 6 corticothalamic cells (269.4 ± 185.9 vs. 50.3 ± 32.9 nC, $P < 0.01$, Mann-Whitney). Similarly, layer 5 corticothalamic neurons showed a larger amount of outward charge transfer than layer 6 corticothalamic neurons (27.2 ± 17.3 vs. 5.2 ± 6.2 nC, $P < 0.025$, Mann-Whitney). We quantitatively compared the spatial distribution of excitatory and inhibitory input with layer 5 corticothalamic and layer 6 corticothalamic cells by determining the number of laser sites producing significant excitation or inhibition, and the lateral expanse of contiguous sites producing excitation or inhibition. We found that layer 5 corticothalamic cells receive a greater degree of both excit-

atory and inhibitory input than layer 6 corticothalamic cells by both measures (number of sites providing excitatory input = 12.9 ± 6.3 for layer 5 vs. 7.3 ± 1.8 for layer 6, $P < 0.025$; number of sites providing inhibitory input = 14.6 ± 5.4 for layer 5 vs. 3.6 ± 3.6 for layer 6, $P = 0.007$; width of excitatory input zone = 386 ± 170 μm for layer 5 vs. 232 ± 80 μm for layer 6, $P = 0.025$; and width of inhibitory input zone = 396 ± 84 μm for layer 5 vs. 182 ± 193 μm for layer 6, $P = 0.021$, all done with Mann-Whitney U -tests). Direct comparisons of the number of activation sites (Fig. 9A) and width of activation zones (Fig. 9B) further demonstrate the larger areas of integration for layer 5 corticothalamic neurons compared with layer 6.

To compare the layer-specific contribution of inputs despite these differences in total synaptic input, we normalized the input based on the total amount of inward or outward charge transfer to a cell (similar to the analysis performed by Briggs and Callaway [2005] and Zarrinpar and Callaway [2006]). Our results for layer-specific inputs, expressed as the percent of total evoked inward or outward synaptic charge transfer that was derived from a specific layer, are shown in Figure 10. As shown in Figure 10A, layer 5 corticothalamic neurons receive approximately $37.2 \pm 33.7\%$ of their excitatory input from layer

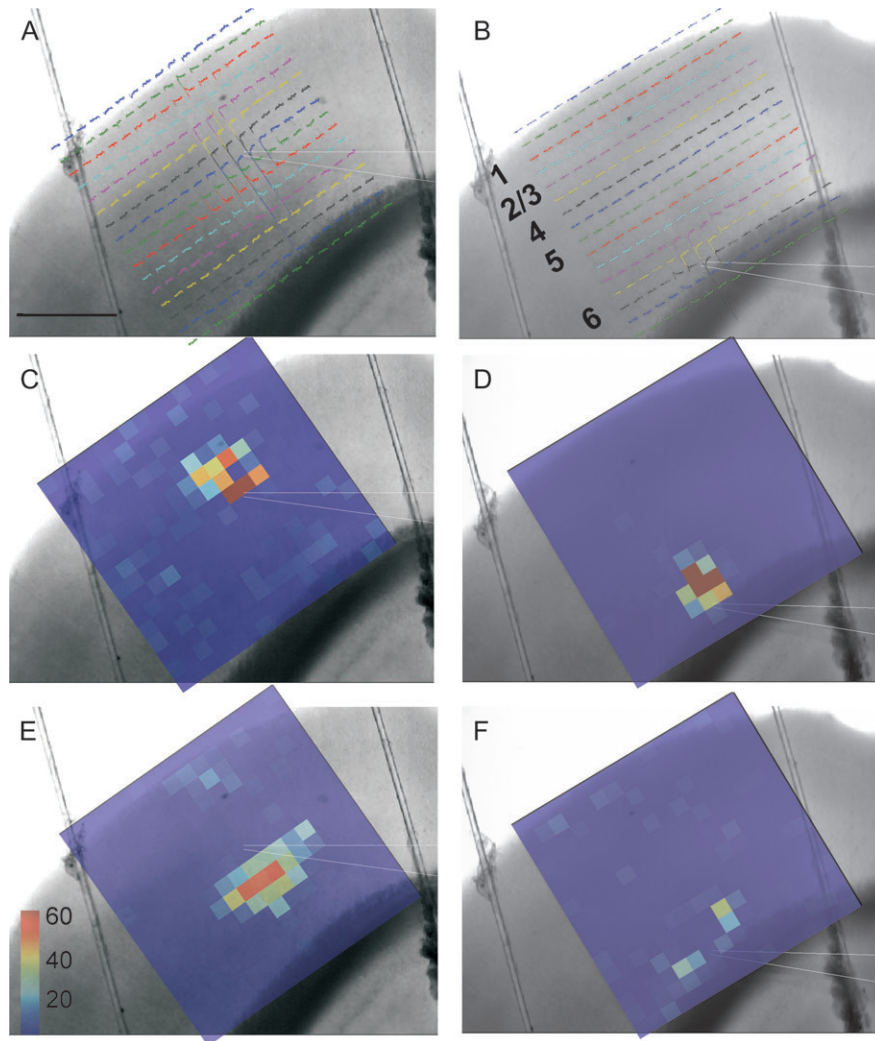


Figure 8. Example of input maps layer 5 and layer 6 corticothalamic neurons residing in vertical register. (*A, B*) Photograph taken at $\times 5$ of the slice while in the recording chamber. Scale bar = $500\ \mu\text{m}$. White dotted lines outline the recording electrode, which was patched onto a layer 5 (*A*) or layer 6 (*B*) corticothalamic cell. Currents recorded from the layer 5 cell (*A*) or layer 6 cell (*B*) held in voltage clamp at $-40\ \text{mV}$ are overlaid. Each of the 256 traces represents the poststimulus current trace in the recorded cell generated by uncaging glutamate at each site. (*C-F*) Pseudocolor maps of the total amount of inward (*C, D*) or outward (*E or F*) charge transfer in a 100-ms window after laser onset. Scale bar units = nanoCoulombs.

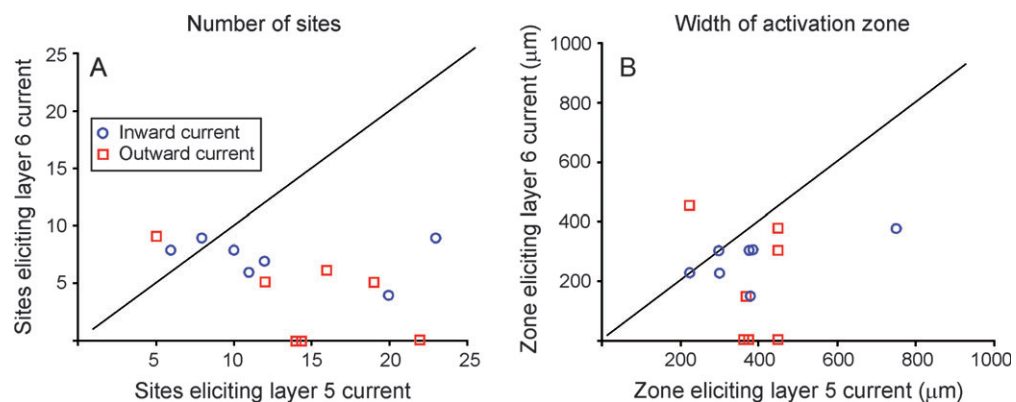


Figure 9. *A*) Scatterplot showing the relationship between the number of photostimulation sites from a 14×14 grid eliciting a significant inward (blue circle) or outward (red square) current for layer 5 and layer 6 corticothalamic neurons from the same cortical column. (*B*) Scatterplot showing the relationship between the horizontal width of the region eliciting a significant inward (blue circle) or outward (red square) current for layer 5 and layer 6 corticothalamic neurons from the same cortical column. In each case, the diagonal line represents unity slope or an equivalent number of sites (*A*) or width of activation zone (*B*) eliciting a response in intracolumnar layer 5 and layer 6 corticothalamic neurons.

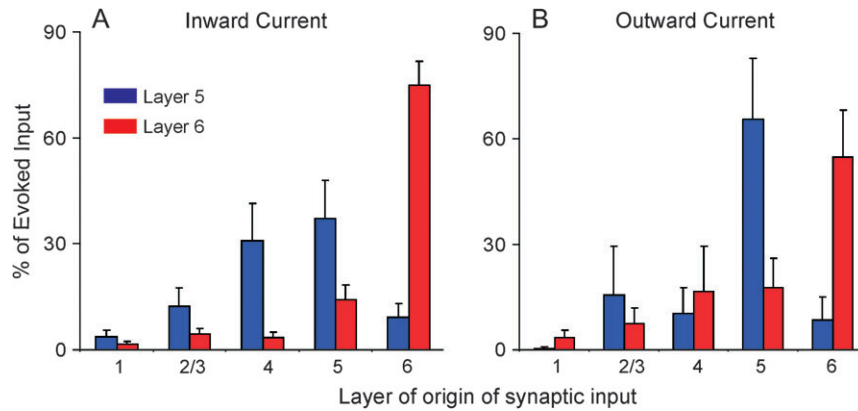


Figure 10. Distribution of inputs to corticothalamic neurons. (A) Percent of total evoked inward charge transfer onto layer 5 corticothalamic cells (blue) and layer 6 corticothalamic cells (red). (B) Percent of total evoked outward charge transfer onto layer 5 corticothalamic cells (blue) and layer 6 corticothalamic cells (red). Error bars represent standard error.

5, $53.6 \pm 25.7\%$ from layers 1–4, and $9.2 \pm 10.6\%$ from layer 6. In contrast, layer 6 corticothalamic cells receive $74.7 \pm 18.2\%$ of their excitatory input from layer 6 and $25.3 \pm 18.2\%$ from all other layers combined. The distributions of inputs were significantly different ($P < 0.0001$, χ^2 -test). We also determined that the percentage of evoked inward synaptic current from outside the home layer of the recorded neuron was larger for layer 5 than layer 6 corticothalamic neurons (layer 5 cells: $62.8 \pm 28.3\%$, layer 6 cells: $25.3 \pm 18.2\%$, $P < 0.025$, Mann-Whitney). The laminar distributions of inhibitory input are shown in Figure 10B. Layer 5 cells received $65.6 \pm 34.5\%$ of their inhibitory input from layer 5, $26.1 \pm 34.7\%$ from layers 1–4, and $8.3 \pm 13.4\%$ from layer 6. In contrast, layer 6 units received $54.8 \pm 26.7\%$ of their inhibitory input from layer 6, and the remainder from all other layers combined. These distributions were also significantly different ($P < 0.0001$, χ^2 -test). There was no difference in the degree of inhibitory input derived from outside of the home layer of the recorded neuron (layer 5 cells: $34.4 \pm 34.5\%$, layer 6 cells: $45.2 \pm 26.7\%$, $P = 0.417$, Mann-Whitney).

Figure 11 displays averaged synaptic input maps and normalized to peak evoked charge transfer for layer 5 and layer 6 corticothalamic neurons. These data confirm that layer 5 corticothalamic neurons have larger excitatory input fields than layer 6 corticothalamic neurons. They also demonstrate that there appears to be a different distribution of inhibitory input to layer 5 and layer 6 corticothalamic cells. Layer 5 cells receive inhibitory input from a wide contiguous band approximately 75–150 μm ventral to the recorded cells, whereas inhibitory input to layer 6 cells is derived from distinct foci approximately 225–300 μm lateral to the recorded cells.

We examined the nature of the inhibition seen in 8 layer 5 and 5 layer 6 corticothalamic neurons. In all cells, and from all stimulation sites, synaptic outward currents were abolished by 1 μM SR 95531 that is a GABA_A receptors blocker, suggesting that all the inhibition that we observed is due to activation of GABA_A receptors (Fig. 12).

Discussion

We have shown that identified adult auditory layer 5 and layer 6 corticothalamic neurons can be distinguished based on morphological properties, intrinsic electrical properties, and

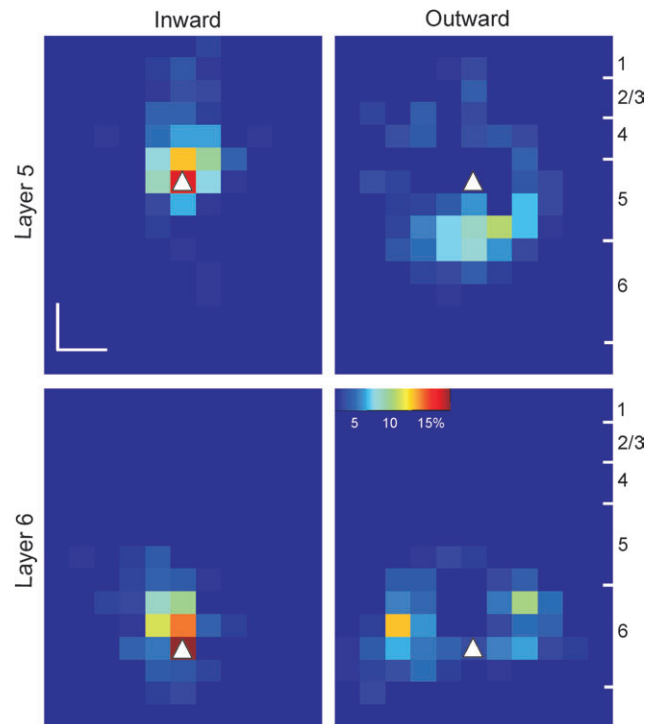


Figure 11. Mean normalized input maps for 7 layer 5 corticothalamic cells (top row) and 7 column-matched layer 6 corticothalamic cells (bottom row) for both inward (left column) and outward total charge transfer (right column). Pseudocolor maps represent the total amount of current entering or exiting a cell in a 100-ms window after a laser pulse at each of the 256 sites. Layer designations computed from mean distance from recorded cell to layer borders directly above or below the cell. Scale bar = 150 μm .

local network input. Specifically, layer 5 corticothalamic neurons are large pyramidal neurons with a thick apical dendrite containing an apical tuft extending into layer 1, whereas layer 6 corticothalamic neurons are small pyramidal neurons with short and thin apical dendrites. We demonstrate that most layer 5 corticothalamic neurons demonstrate developmentally dependent bursting in response to depolarizing current pulses, whereas layer 6 corticothalamic neurons demonstrate a regular spiking. Further, we used photostimulation in identified neurons to demonstrate that layer 5

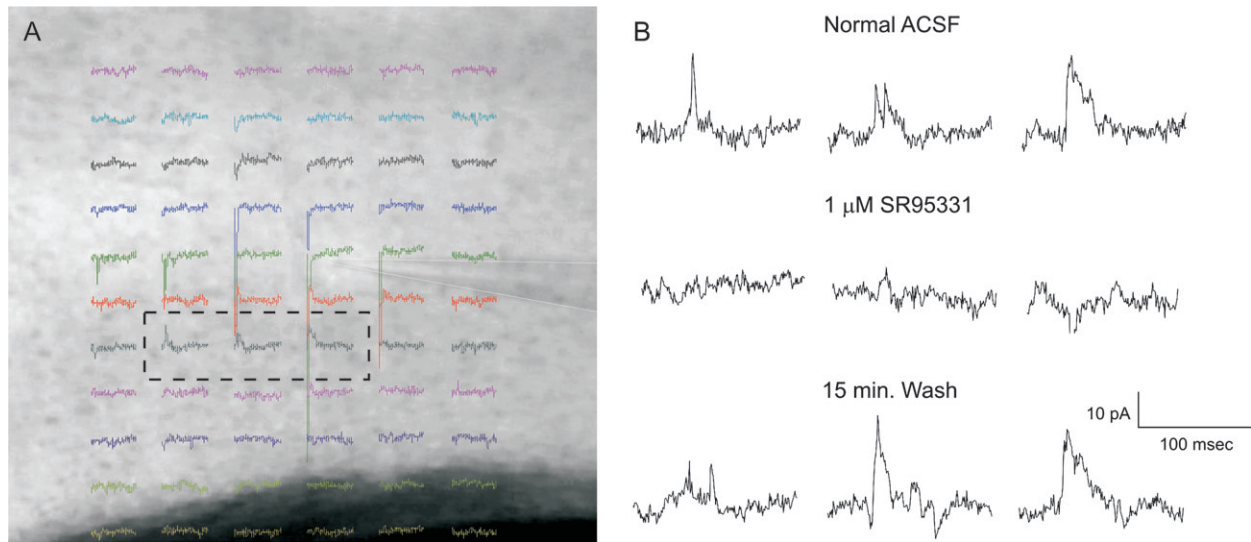


Figure 12. Blockade of outward currents with bath-applied SR 9531, a GABA_A receptor blocker, at 1 μ M. (A) Subset of currents recorded in voltage clamp at -40 mV of a layer 5 corticothalamic neuron (electrode outlined in white). Outward currents are seen in lower layer 5. (B) Expanded view of currents from 3 sites in black dashed box in (A), predrug (top), during drug (middle), and postwash (bottom).

corticothalamic neurons integrate excitatory inputs over a significantly larger area and across more layers than do coregistered layer 6 corticothalamic neurons and that the patterns of GABA_Aergic inhibition differ between these 2 cell types. Herein, we discuss the implications of these findings with respect to the distinct roles potentially played by layer 5 and layer 6 corticothalamic projections.

Morphology Comparison

The current morphologic findings in layer 5 corticothalamic neurons that project to the higher order portions of the auditory thalamus are similar to what has been seen in intrinsic bursting layer 5 corticothalamic neurons in the auditory, visual, and somatosensory systems (Schofield et al. 1987; Chagnac-Amitai et al. 1990; Larkman and Mason 1990; Kasper et al. 1994; Hefti and Smith 2000; Hattox and Nelson 2007). Because many inputs to layer 1 are comprised of fibers from distant cortical areas and long-range thalamocortical axonal branches, it is possible that layer 5 corticothalamic neurons integrate information from distant sources with local inputs from layers 2/3, 4, or 5 (Cauller et al. 1998; Cetas et al. 1999; Oda et al. 2004). Indeed, it has been proposed that such dendritic morphology, coupled with active dendritic calcium conductances (see below), allows these neurons to serve as coincidence detectors for upper and middle layer input (Larkum, Zhu, et al. 1999; Llinas et al. 2002).

We found that most layer 6 corticothalamic neurons had small pyramidal morphology and had apical dendrites that rarely extended above layer 4. Similar characteristics have been seen in layer 6 of the cat auditory cortex (Ojima et al. 1992; Prieto and Winer 1999) in layer 6 corticothalamic neurons in the rat barrel cortex (Zhang and Deschenes 1997) and in lateral geniculate-projecting neurons in layer 6 of the tree shrew and cat visual cortices (Katz 1987; Usrey and Fitzpatrick 1996). Unlike Usrey and Fitzpatrick, who described branched supragranular layer-projecting axons from corticopulvinar layer 6 neurons, we did not observe extensive intracortical axonal branching. Our injections typically involved the dorsal division

of the medial geniculate body, which projects to the non-primary auditory cortex (Winer et al. 1999) and is considered to be a higher order nucleus analogous to the pulvinar (Llano and Sherman 2008). Therefore, one might have expected that some of the layer 6 neurons in the current study to have the morphology of the corticopulvinar neurons seen in Usrey and Fitzpatrick. This difference may be related to the relatively small sample size of the current study or species-related or sensory system-related differences.

Physiology Comparison

We found low-threshold bursting in the majority of layer 5 corticothalamic neurons, which is consistent with what has been seen in adult brainstem- and midbrain-projecting neurons in the sensorimotor and visual cortex. The mechanism underlying bursting has been studied by several investigators (Friedman and Gutnick 1989; Markram Sakmann 1994; Franceschetti et al. 1995; Larkum, Kaiser, et al. 1999; Larkum, Zhu, et al. 1999; Schwindt and Crill 1999) who have found that such bursting is likely created by a dendritic low-threshold voltage-dependent calcium current with a possible contribution of persistent voltage-dependent sodium current. The calcium current can be triggered by a backpropagating sodium action potential from the soma, which serves as the basis for a proposed coincidence detection mechanism by these neurons (Larkum, Zhu, et al. 1999). Schwindt and Crill (1999) found that dendritic depolarization with glutamate, coupled with somatic depolarization, was able to convert regular spiking large layer 5 pyramidal cells into cells that displayed bursting in response to somatic depolarization. This finding raises the possibility that regular spiking layer 5 corticothalamic neurons may be convertible into bursting neurons if dendritic depolarization is coupled with somatic depolarization. This proposal is supported by the finding that regular spiking layer 5 corticothalamic neurons shared the same morphological (dendritic tuft) and electrophysiological (prominent DAP) characteristics as their bursting counterparts. These data suggest that the absence in bursting seen in these neurons may be related to an unmeasured parameter, such as dendritic branching, or possibly to

damage, coupled with large electrotonic size of these neurons, such that somatic current injection did not permit adequate dendritic depolarization to achieve bursting.

We were able to convert bursting into regular spiking responses by predepolarizing the soma by injection of depolarizing somatic current (Fig. 5E,F). This phenomenon is consistent with findings from Wang and McCormick (1993) who found that depolarization with norepinephrine, the non-specific metabotropic glutamate receptor agonist ACPD or acetylcholine converted layer 5 bursting responses into regular spiking responses and with Schwindt et al. (1997) who found that bursting layer 5 cells did not burst in response to slow depolarizing ramps. In the present study, the degree of dendritic depolarization caused by somatic current injection is likely to be small, given the large electrotonic size of these neurons (Larkman et al. 1992). It is also not clear whether bursting was inhibited by the tonic voltage change during the prepulse or the action potentials present during the prepulse. Previous work has yielded conflicting results on this issue. Imaging of dendritic calcium transients in layer 5 pyramidal cells during repetitive short-duration somatic stimulation did not show decay of the calcium signal at high stimulation rates (>100 Hz; Larkum, Kaiser, et al. 1999). In contrast, in the rabbit visual cortex *in vivo*, backpropagating action potential signal amplitude significantly decreased with repetitive axonal stimulation and amplitude began to drop off at interpulse intervals of approximately 50 ms (Bereshpolova et al. 2007), which is on the order of the 50% drop-off rate for the paired-pulse data from the current study (Fig. 5D; 50% drop-off point = 89.6 ± 57 ms). The absence of signal drop-off in the Larkum, Kaiser, et al. study may be related to lack of tonic depolarization, which is necessary to inactivate other voltage- and time-dependent calcium currents, such as the T-current (Jahnsen and Llinas 1984), whereas it is possible that the antidromic stimulation in the Bereshpolova et al. (2007) study caused network activity leading to tonic depolarization of layer 5 neurons (see their Fig. 2A).

Biphasic afterpotentials with a prominent DAP were found in nearly all layer 5 corticothalamic neurons, even after spikes outside of bursts (see latter spikes in Fig. 2D). This finding suggests that the DAP may be an attenuated version of the calcium current underlying a burst and that regular spiking neurons displaying a large DAP may be convertible into a bursting mode. It is also important to add that the ability for bursting neurons to be converted into regular spiking neurons (current study) and for regular spiking neurons to be converted into bursting neurons (Schwindt and Crill 1999) by manipulation of membrane voltage and the timing and spatial location of inputs suggests that bursting in these neurons may be an important signaling mechanism that is under tight physiological control.

Similar to previous work in rats (Kasper et al. 1994), we found that bursting in layer 5 corticothalamic neurons is age-dependent. We also found that juvenile and adult layer 5 bursting neurons could be differentiated based on the smaller input resistance (suggesting a larger size) and larger DAP in adult neurons (Table 2). In addition, the DAP amplitude was largest in layer 5 corticothalamic neurons compared with all other groups tested (Fig. 6). Because the DAP is thought to be calcium-dependent (Friedman and Gutnick 1989; Mason and Larkman 1990; Friedman et al. 1992), these data suggest that the developmental dependence of bursting may be related to the development of the DAP, possibly located on the apical

dendrite, which also undergoes significant postnatal developmental maturation (Zhang 2004).

Another significant difference between layer 5 and layer 6 corticothalamic neurons was the prominence of I_h in layer 5. Prominent I_h has been demonstrated previously in other studies of subcortically projecting layer 5 neurons (Kasper et al. 1994; Christophe et al. 2005). The significance of I_h for these neurons is not known, though activation of this current may be responsible for the relatively depolarized resting potential observed in these cells because the reversal potential for I_h is in the range of -17 to -40 mV (McCormick and Pape 1990; Maccaferri et al. 1993). I_h in cortical pyramidal neurons has also been postulated to be important for the generation of persistent activity (Winograd et al. 2008) and/or uncoupling somatic and dendritic activation (Stuart and Spruston 1998; Berger et al. 2003), which enhances their ability to serve as coincidence detectors (Berger et al. 2003).

Layer 6 corticothalamic neurons did not demonstrate bursting, displayed prominent fAHPs, and had more adaptation and similar terminal spike rates as their layer 5 counterparts. A similar combination of findings has been seen in CA1 pyramidal neurons and has been attributed to activation of a BK-type potassium channel (Gu et al. 2007). Other investigators have also reported that layer 6 corticothalamic neurons show regular spiking (Brumberg et al. 2003; Mercer et al. 2005), though these groups differed in their findings regarding spike frequency adaptation. The significance of spike frequency adaptation in the context of relatively high firing rates is not clear. We have shown that layer 6 corticothalamic activation can elicit paired-pulse facilitation at rates of 10–15 Hz (Reichova and Sherman 2004). The average firing rate in our layer 6 corticothalamic neurons (measured at 200 pA above threshold) was well above 10–15 Hz (average firing rate at the end of 400 ms = 25.4 ± 8.5 Hz), suggesting that layer 6 corticothalamic neurons individually may elicit facilitation at corticothalamic synapses.

Input Maps

Compared with layer 6 corticothalamic neurons, we found that layer 5 corticothalamic cells receive a substantial proportion of their local excitatory input from layers outside of their home layer. We also found that the tangential width and number of sites eliciting an excitatory response for these neurons exceeded those for layer 6 corticothalamic neurons. These results were expected given the larger somatic and apical dendritic size seen in layer 5 corticothalamic cells. Our results regarding layer 5 neurons are generally consistent with those of Schubert et al. (2001), who used photostimulation to create synaptic input maps of intrinsic bursting layer 5 neurons from the barrel cortex. These authors showed widespread synaptic inputs from layers 2–6, both from the home and neighboring barrels. However, their data also revealed a greater degree of input from layer 6 as well as significantly less inhibitory input than our data. In addition, in a photostimulation study of layer 5 neurons of the monkey visual cortex, multiple types of input maps were observed, with very little inhibitory input. Excitatory input was derived from layers 2–6, with clusters that were enriched with pyramidal cells having a greater degree of input from layers 2–4B (Briggs and Callaway 2005). One source of the discrepancy between our data and the previous 2

photostimulation studies is that we distinguished between direct and synaptic activation by subtracting the input map generated in synaptic blockade from the total input map. This approach is in contrast to the Schubert et al. (2001) and Briggs and Callaway (2005) studies, which used a 10- and 2-ms window, respectively, to distinguish between direct and synaptic activation. We believe that our method offers significant advantages because it removes assumptions about the timing of synaptic activation. Timing windows may eliminate early synaptic responses from nearby neurons, deemphasizing inputs from local contacts. Timing windows may also include direct inputs from distal dendrites with a long rise time, overemphasizing distant contacts. This methodological difference may account for our findings, which show a greater proportion of local inputs than others have found for layer 5 neurons.

Similarly, we found a relatively homogenous population of layer 6 input maps, with most neurons receiving only local excitatory input. This finding is similar to what was seen using photostimulation in presumed layer 6 corticothalamic neurons in the rat visual cortex (Zarrinpar and Callaway 2006). Here, only layer 6 inhibitory interneurons had significant supragranular input. The same group, however, found significant supragranular input to monkey visual cortical layer 6 pyramidal cells, which may be related to species' differences (Briggs and Callaway 2001). Our finding of restricted local inputs to layer 6 corticothalamic neurons is supported by data showing that nonthalamic-projecting layer 6 neurons have a more widespread dendritic arborization and larger dendritic areas than their thalamic-projecting neighbors (Ojima et al. 1992; Zhang and Deschenes 1997; Brumberg et al. 2003).

A surprising finding is the presence of widespread GABA_A-ergic inhibitory input onto layer 5 corticothalamic cells, which derived from layer 2/3 and lower layer 5. Hefti and Smith (2000) found that layer 5 regular spiking cells had a significantly greater degree of inhibitory input than intrinsic bursting cells when stimulating the subcortical white matter. In addition, *in vivo*, Turner et al. (2005) found that presumed intrinsic bursting neurons in the auditory cortex had wide tuning curves and were easily drivable with external sources of current, in contrast to presumed layer 5 regular spiking cells which were difficult to drive and had smaller response areas. Similar observations were made in layer 5 of motor cortex (Sirota et al. 2005). Other laser mapping studies of layer 5 neurons did not find significant inhibition likely because they were held at potentials close enough to the chloride equilibrium potential to prevent observation of outward currents (Schubert et al. 2001; Briggs and Callaway 2005). It is possible that inhibition is latent and not elicitable by simple acoustic stimulation or by electrical stimulation of the subcortical white matter. Inhibition may only be elicitable via corticocortical interactions or potentially via long-range cholinergic inputs (Beaulieu and Somogyi, 1991; Kawaguchi 1997). Because we have shown that bursting may be eliminated by suprathreshold predepolarization, inhibition may play an important role in offsetting external excitation to maintain layer 5 corticothalamic neurons in a "burst mode." Alternatively, inhibition may be important for synchronizing neural outputs (Galarreta and Hestrin 2001), which is consistent with the proposal that layer 5 bursting neurons promote cortical synchronization (Chagnac-Amitai and Connors 1989).

Unlike the contiguous band of inhibitory input impinging onto layer 5 corticothalamic neurons, inhibitory input onto

layer 6 corticothalamic neurons was derived from discrete foci located approximately 225–300 μm to either side of the recorded neuron. This type of transcolumar inhibition has not been previously described for layer 6 neurons and could serve as a substrate for lateral inhibition, which has been extensively documented in the auditory cortex (Calford and Semple 1995; Sutter et al. 1999; Ojima and Murakami 2002). Note that this inhibition would likely be for a dimension other than frequency tuning because murine coronal slices (as in this study) are likely cut along isofrequency contours (Stiebler et al. 1997).

Driver and Modulator Functions

The voltage and time dependence of bursts suggest that, similar to thalamocortical bursts (Ramcharan et al. 2005), layer 5 corticothalamic bursts may be more likely to occur after a period of relative quiescence. Furthermore, both thalamocortical and corticothalamic bursts are transmitted through a depressing synapse (Castro-Alamancos and Connors 1997; Gil et al. 1999; Reichova and Sherman 2004). In the case of layer 5 corticothalamic synapses, the average time needed to recover bursting after a previous burst is approximately 90 ms (Fig. 5D), which is an interpulse interval that would allow substantial recovery of short-term depression observed at these synapses (Groh et al. 2008; Reichova and Sherman 2004). Therefore, similar to the thalamocortical system (Swadlow and Gusev 2001), the temporal firing properties of the layer 5 corticothalamic projections

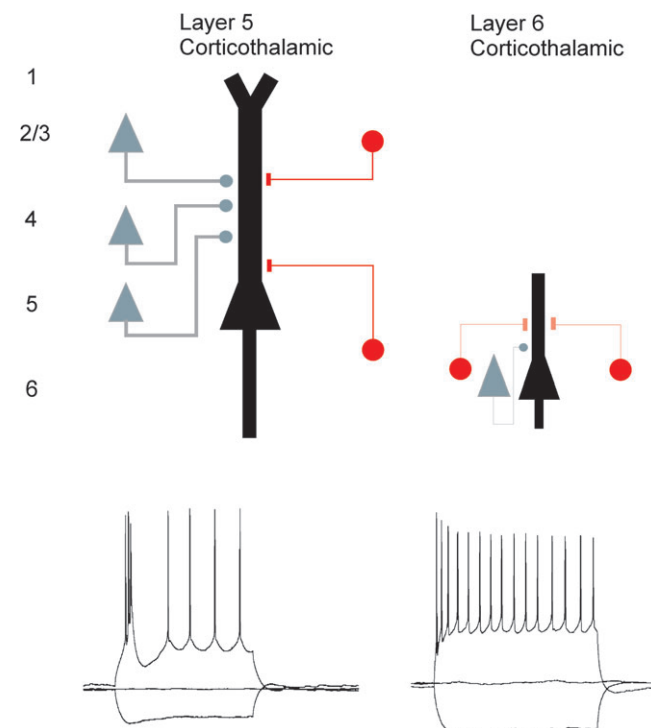


Figure 13. Proposed model of differences of synaptic input and response properties between auditory layer 5 and layer 6 corticothalamic neurons. In our model, layer 5 corticothalamic neurons receive excitatory input from neurons in layers 2/3, 4, and 5 (gray) and GABA_A-mediated inhibitory input mostly from lower layer 5 with a smaller contribution from layer 2/3 (red). In response to excitatory input, these neurons fire a burst of action potentials at low threshold. In contrast, layer 6 corticothalamic neurons integrate excitatory input primarily from layer 6 and receive inhibitory input from adjacent areas in layer 6. In response to excitatory input, these neurons fire a train of individual action potentials.

are suited for maximum synaptic efficacy. Likewise, the relatively high firing rates of layer 6 corticothalamic neurons induced by depolarization would be poorly suited for a driver corticothalamic synapse, which would filter out much of the information in the spike train, but well suited for modulator corticothalamic synapses, where paired-pulse facilitation and metabotropic glutamate receptor activation are found.

Summary and Conclusions

Figure 13 illustrates a model to summarize our main results. Our data suggest that layer 5 corticothalamic neurons are large, bursting neurons with apical dendrites extending into layer 1 and that they receive excitatory input from a relatively wide area from layers 2/3, 4, and 5, with inhibitory input from a wide area of layers 2/3 (weaker) and lower layer 5 (stronger). In contrast, layer 6 corticothalamic neurons are smaller pyramidal cells that demonstrate a regular spiking profile, receive local excitatory, and discrete transcolumar inhibitory input.

The current findings delineating the differences between layer 5 and layer 6 corticothalamic neurons support and extend the idea that each of these layers has a distinct role in corticothalamocortical communication. Layer 5 neurons bear a stronger resemblance to layer 5 neurons that project to other subcortical targets than to their layer 6 corticothalamic counterparts, suggesting that layer 5 corticofugal neurons are part of a wider system with distinct physiological properties. In the current context, layer 5 corticothalamic neurons, as drivers, integrate information over a large area of cortex and relay a highly secure signal, in the form of a burst, to their higher order thalamic targets. Layer 6 neurons, as modulators, integrate information locally, perhaps receiving input from the thalamus (Adams and Cox 2002; Briggs and Usrey 2007), and have spike train characteristics that are appropriate to modulate the excitability of their postsynaptic thalamic targets. Further work will elucidate the functional roles of the 2 distinct systems described here.

Funding

United States Public Health Service, National Institutes of Health (DC008320 to D.A.L.; EY03038 and DC008794 to S.M.S.).

Notes

The authors thank Charles C. Lee and Brian T. Theyel for their comments on the manuscript. *Conflict of Interest:* None declared.

Address correspondence to Daniel A. Llano, Departments of Neurology and Neurobiology, University of Chicago, 947 East 58th Street, MC0926 316 Abbott, Chicago, IL 60637, USA. Email: a.daniel.llano@gmail.com.

References

Adams P, Cox K. 2002. A new interpretation of thalamocortical circuitry. *Philos Trans R Soc Lond B Biol Sci.* 357:1767-1779.

Beaulieu C, Somogyi P. 1991. Enrichment of cholinergic synaptic terminals on GABAergic neurons and coexistence of immunoreactive GABA and choline acetyltransferase in the same synaptic terminals in the striate cortex of the cat. *J Comp Neurol.* 304: 666-680.

Berespolova Y, Amitai Y, Gusev AG, Stoelzel CR, Swadlow HA. 2007. Dendritic backpropagation and the state of the awake neocortex. *J Neurosci.* 27:9392-9399.

Berger T, Senn W, Luscher H-R. 2003. Hyperpolarization-activated current Ih disconnects somatic and dendritic spike initiation zones in layer V pyramidal neurons. *J Neurophysiol.* 90:2428-2437.

Briggs F, Callaway EM. 2001. Layer-specific input to distinct cell types in layer 6 of monkey primary visual cortex. *J Neurosci.* 21:3600-3608.

Briggs F, Callaway EM. 2005. Laminar patterns of local excitatory input to layer 5 neurons in macaque primary visual cortex. *Cereb Cortex.* 15:479-488.

Briggs F, Usrey WM. 2007. A fast, reciprocal pathway between the lateral geniculate nucleus and visual cortex in the macaque monkey. *J Neurosci.* 27:5431-5436.

Brumberg JC, Hamzei-Sichani F, Yuste R. 2003. Morphological and physiological characterization of layer VI corticofugal neurons of mouse primary visual cortex. *J Neurophysiol.* 89:2854-2867.

Calford MB, Semple MN. 1995. Monaural inhibition in cat auditory cortex. *J Neurophysiol.* 73:1876-1891.

Castelo-Branco M, Neuenschwander S, Singer W. 1998. Synchronization of visual responses between the cortex, lateral geniculate nucleus, and retina in the anesthetized cat. *J Neurosci.* 18:6395-6410.

Castro-Alamancos MA, Connors BW. 1997. Thalamocortical synapses. *Prog Neurobiol.* 51:581-606.

Caulier LJ, Clancy B, Connors BW. 1998. Backward cortical projections to primary somatosensory cortex in rats extend long horizontal axons in layer I. *J Comp Neurol.* 390:297-310.

Cetas JS, de Venecia RK, McMullen NT. 1999. Thalamocortical afferents of Lorente de N6: medial geniculate axons that project to primary auditory cortex have collateral branches to layer I. *Brain Res.* 830:203-208.

Chagnac-Amitai Y, Connors BW. 1989. Synchronized excitation and inhibition driven by intrinsically bursting neurons in neocortex. *J Neurophysiol.* 62:1149-1162.

Chagnac-Amitai Y, Luhmann HJ, Prince DA. 1990. Burst generating and regular spiking layer 5 pyramidal neurons of rat neocortex have different morphological features. *J Comp Neurol.* 296:598-613.

Christophe E, Doerflinger N, Lavery DJ, Molnar Z, Chrapak S, Audinat E. 2005. Two populations of layer V pyramidal cells of the mouse neocortex: development and sensitivity to anesthetics. *J Neurophysiol.* 94:3357-3367.

Connors BW, Gutnick MJ, Prince DA. 1982. Electrophysiological properties of neocortical neurons in vitro. *J Neurophysiol.* 48: 1302-1320.

Deschênes M, Bourassa J, Pinault D. 1994. Corticothalamic projections from layer V cells in rat are collaterals of long-range corticofugal axons. *Brain Res.* 664:215-219.

Franceschetti S, Guatteo E, Panzica F, Sancini G, Wanke E, Avanzini G. 1995. Ionic mechanisms underlying burst firing in pyramidal neurons: Intracellular study in rat sensorimotor cortex. *Brain Res.* 696:127-139.

Friedman A, Arens J, Heinemann U, Gutnick MJ. 1992. Slow depolarizing afterpotentials in neocortical neurons are sodium and calcium dependent. *Neurosci Lett.* 135:13-17.

Friedman A, Gutnick MJ. 1989. Intracellular calcium and control of burst generation in neurons of guinea-pig neocortex in vitro. *European Journal of Neuroscience.* 1:374-381.

Galarreta M, Hestrin S. 2001. Spike transmission and synchrony detection in networks of GABAergic interneurons. *Science.* 292:2295-2299.

Gil Z, Connors BW, Amitai Y. 1999. Efficacy of thalamocortical and intracortical synaptic connections: quanta, innervation, and reliability. *Neuron.* 23:395-397.

Groh A, de Kock CPJ, Wimmer VC, Sakmann B, Kuner T. 2008. Driver or coincidence detector: modal switch of a corticothalamic giant synapse controlled by spontaneous activity and short-term depression. *J Neurosci.* 28:9652-9663.

Gu N, Vervaeke K, Storm JF. 2007. BK potassium channels facilitate high-frequency firing and cause early spike frequency adaptation in rat CA1 hippocampal pyramidal cells. *J Physiol.* 580:859-882.

Hattox AM, Nelson SB. 2007. Layer V neurons in mouse cortex projecting to different targets have distinct physiological properties. *J Neurophysiol.* 98:3330-3340.

Hefti BJ, Smith PH. 2000. Anatomy, physiology, and synaptic responses of rat layer V auditory cortical cells and effects of intracellular GABAA blockade. *J Neurophysiol.* 83:2626-2638.

- Hoogland PV, Welker E, Van der Loos H. 1987. Organization of the projections from barrel cortex to thalamus in mice studied with Phaseolus vulgaris-leucoagglutinin and HRP. *Exp Brain Res*. 68:73-87.
- Jahnsen H, Llinas R. 1984. Electrophysiological properties of guinea-pig thalamic neurones: an in vitro study. *J Physiol*. 349:205-226.
- Jones EG. 2002. Thalamic circuitry and thalamocortical synchrony. *Philos Trans R Soc Lond B Biol Sci*. 357:1659-1673.
- Kasper EM, Larkman AU, Lübke J, Blakemore C. 1994. Pyramidal neurons in layer 5 of the rat visual cortex. I. Correlation among cell morphology, intrinsic electrophysiological properties, and axon targets. *J Comp Neurol*. 339:459-474.
- Katz LC. 1987. Local circuitry of identified projection neurons in cat visual cortex brain slices. *J Neurosci*. 7:1223-1249.
- Katz LC, Dalva MB. 1994. Scanning laser photostimulation: a new approach for analyzing brain circuits. *J Neurosci Methods*. 54(2):205-218.
- Kawaguchi Y. 1997. Selective cholinergic modulation of cortical GABAergic cell subtypes. *J Neurophysiol*. 78:1743-1747.
- Lam Y-W, Sherman SM. 2005. Mapping by laser photostimulation of connections between the thalamic reticular and ventral posterior lateral nuclei in the rat. *J Neurophysiol*. 94:2472-2483.
- Larkman A, Mason A. 1990. Correlations between morphology and electrophysiology of pyramidal neurons in slices of rat visual cortex. I. Establishment of cell classes. *J Neurosci*. 10:1407-1414.
- Larkman AU, Major G, Stratford K, Jack JJB. 1992. Dendritic morphology of pyramidal neurones of the visual cortex of the rat. IV: electrical geometry. *J Comp Neurol*. 323:137-152.
- Larkum ME, Kaiser KMM, Sakmann B. 1999. Calcium electrogenesis in distal apical dendrites of layer 5 pyramidal cells at a critical frequency of back-propagating action potentials. *Proc Natl Acad Sci USA*. 96:14600-14604.
- Larkum ME, Zhu JJ, Sakmann B. 1999. A new cellular mechanism for coupling inputs arriving at different cortical layers. *Nature*. 398:338-341.
- Le Be J-V, Silberberg G, Wang Y, Markram H. 2007. Morphological, electrophysiological, and synaptic properties of corticocortical pyramidal cells in the neonatal rat neocortex. *Cereb Cortex*. 17:2204-2213.
- Lisman JE. 1997. Bursts as a unit of neural information: making unreliable synapses reliable. *Trends Neurosci*. 20(1):38-43.
- Llano DA, Sherman SM. 2008. Evidence for nonreciprocal organization of the mouse auditory thalamocortical-corticothalamic projection systems. *J Comp Neurol*. 507:1209-1227.
- Llinas RR, Leznik E, Urbano FJ. 2002. Temporal binding via cortical coincidence detection of specific and nonspecific thalamocortical inputs: a voltage-dependent dye-imaging study in mouse brain slices. *Proc Natl Acad Sci USA*. 99:449-454.
- Maccaferri G, Mangoni M, Lazzari A, DiFrancesco D. 1993. Properties of the hyperpolarization-activated current in rat hippocampal CA1 pyramidal cells. *J Neurophysiol*. 69:2129-2136.
- Markram H, Sakmann B. 1994. Calcium transients in dendrites of neocortical neurons evoked by single subthreshold excitatory postsynaptic potentials via low-voltage-activated calcium channels. *Proc Natl Acad Sci USA*. 11:5207-5211.
- Mason A, Larkman A. 1990. Correlations between morphology and electrophysiology of pyramidal neurons in slices of rat visual cortex. II. Electrophysiology. *J Neurosci*. 10:1415-1428.
- McCormick DA, Pape HC. 1990. Properties of a hyperpolarization-activated cation current and its role in rhythmic oscillation in thalamic relay neurones. *J Physiol*. 431:291-318.
- Meltzer NE, Ryugo DK. 2006. Projections from auditory cortex to cochlear nucleus: a comparative analysis of rat and mouse. *Anat Rec A Discov Mol Cell Evol Biol*. 288A:397-408.
- Mercer A, West DC, Morris OT, Kirchhecker S, Kerkhoff JE, Thomson AM. 2005. Excitatory connections made by presynaptic cortico-cortical pyramidal cells in layer 6 of the neocortex. *Cereb Cortex*. 15:1485-1496.
- Oda S, Kishi K, Yang J, Chen S, Yokofujita J, Igarashi H, Tanihata S, Kuroda M. 2004. Thalamocortical projection from the ventral posteromedial nucleus sends its collaterals to layer I of the primary somatosensory cortex in rat. *Neurosci Lett*. 367:394-398.
- Ojima H. 1994. Terminal morphology and distribution of corticothalamic fibers originating from layers 5 and 6 of cat primary auditory cortex. *Cereb Cortex*. 4:646-663.
- Ojima H, Honda CN, Jones EG. 1992. Characteristics of intracellularly injected infragranular pyramidal neurons in cat primary auditory cortex. *Cereb Cortex*. 2:197-216.
- Ojima H, Murakami K. 2002. Intracellular characterization of suppressive responses in supragranular pyramidal neurons of cat primary auditory cortex in vivo. *Cereb Cortex*. 12:1079-1091.
- Prieto JJ, Winer JA. 1999. Layer VI in cat primary auditory cortex: golgi study and sublaminar origins of projection neurons. *J Comp Neurol*. 404:332-358.
- Ramcharan EJ, Gnadt JW, Sherman SM. 2005. Higher-order thalamic relays burst more than first-order relays. *Proc Natl Acad Sci USA*. 102:12236-12241.
- Ramos RL, Tam DM, Brumberg JC. 2008. Physiology and morphology of callosal projection neurons in mouse. *Neuroscience*. 153:654-663.
- Reichova I, Sherman SM. 2004. Somatosensory corticothalamic projections: distinguishing drivers from modulators. *J Neurophysiol*. 92:2185-2197.
- Rouiller EM, Durif C. 2004. The dual pattern of corticothalamic projection of the primary auditory cortex in macaque monkey. *Neurosci Lett*. 358:49-52.
- Rouiller EM, Welker E. 1991. Morphology of corticothalamic terminals arising from the auditory cortex of the rat: a Phaseolus vulgaris-leucoagglutinin (PHA-L) tracing study. *Hear Res*. 56:179-190.
- Rumberger A, Schmidt M, Lohmann H, Hoffman K. 1998. Correlation of electrophysiology, morphology, and functions in corticotectal and corticopretectal projection neurons in rat visual cortex. *Exp Brain Res*. 119:375-390.
- Schofield BR, Hallman LE, Lin CS. 1987. Morphology of corticotectal cells in the primary visual cortex of hooded rats. *J Comp Neurol*. 261:85-97.
- Schubert D, Kotter R, Luhmann HJ, Staiger JF. 2006. Morphology, electrophysiology and functional input connectivity of pyramidal neurons characterizes a genuine layer Va in the primary somatosensory cortex. *Cereb Cortex*. 16:223-236.
- Schubert D, Staiger JF, Cho N, Kotter R, Zilles K, Luhmann HJ. 2001. Layer-specific intracolumnar and transcolumar functional connectivity of layer V pyramidal cells in rat barrel cortex. *J Neurosci*. 21:3580-3592.
- Schwandt P, Crill W. 1999. Mechanisms underlying burst and regular spiking evoked by dendritic depolarization in layer 5 cortical pyramidal neurons. *J Neurophysiol*. 81:1341-1354.
- Schwandt P, O'Brien JA, Crill W. 1997. Quantitative analysis of firing properties of pyramidal neurons from layer 5 of rat sensorimotor cortex. *J Neurophysiol*. 77:2484-2498.
- Shepherd GMG, Pologruto TA, Svoboda K. 2003. Circuit analysis of experience-dependent plasticity in the developing rat barrel cortex. *Neuron*. 38:277-289.
- Sherman SM. 2007. The thalamus is more than just a relay. *Curr Opin Neurobiol*. 17:417-422.
- Sherman SM, Guillery RW. 1998. On the actions that one nerve cell can have on another: distinguishing "drivers" from "modulators". *Proc Natl Acad Sci USA*. 95:7121-7126.
- Sherman SM, Guillery RW. 2002. The role of the thalamus in the flow of information to the cortex. *Philos Trans R Soc Lond B Biol Sci*. 357:1695-1708.
- Sillito AM, Cudeiro J, Jones HE. 2006. Always returning: feedback and sensory processing in visual cortex and thalamus. *Trends Neurosci*. 29:307-316.
- Sirota MG, Swadlow HA, Beloozerova IN. 2005. Three channels of corticothalamic communication during locomotion. *J Neurosci*. 25:5915-5925.
- Stiebler I, Neulist R, Fichtel I, Ehret G. 1997. The auditory cortex of the house mouse: left-right differences, tonotopic organization and quantitative analysis of frequency representation. *J Comp Physiol A Neuroethol Sens Neural Behav Physiol*. 181:559-571.
- Stuart G, Spruston N. 1998. Determinants of voltage attenuation in neocortical pyramidal neuron dendrites. *J Neurosci*. 18:3501-3510.

- Suga N, Ma X. 2003. Multiparametric corticofugal modulation and plasticity in the auditory system. *Nat Rev Neurosci.* 4:783-794.
- Sutter ML, Schreiner CE, McLean M, O'Connor KN, Loftus WC. 1999. Organization of inhibitory frequency receptive fields in cat primary auditory cortex. *J Neurophysiol.* 82:2358-2371.
- Swadlow HA, Gusev AG. 2001. The impact of 'bursting' thalamic impulses at a neocortical synapse. *Nat Neurosci.* 4:402-408.
- Turner JG, Hughes LF, Caspary DM. 2005. Divergent response properties of layer-V neurons in rat primary auditory cortex. *Hear Res.* 202:129-140.
- Usrey WM, Fitzpatrick D. 1996. Specificity in the axonal connections of layer VI neurons in tree shrew striate cortex: evidence for distinct granular and supragranular systems. *J Neurosci.* 16:1203-1218.
- Van Horn SC, Erisir A, Sherman SM. 2000. Relative distribution of synapses in the A-laminae of the lateral geniculate nucleus of the cat. *J Comp Neurol.* 416:509-520.
- Van Horn SC, Sherman SM. 2004. Differences in projection patterns between large and small corticothalamic terminals. *J Comp Neurol.* 475:406-415.
- Wang Z, McCormick DA. 1993. Control of firing mode of corticotectal and corticopontine layer V burst-generating neurons by norepinephrine, acetylcholine, and 1S,3R-ACPD. *J Neurosci.* 13:2199-2216.
- Wilson JR, Friedlander MJ, Sherman SM. 1984. Fine structural morphology of identified X- and Y-cells in the cat's lateral geniculate nucleus. *Proc R Soc Lond B Biol Sci.* 221:411-436.
- Winer JA, Sally SL, Larue DT, Kelly JB. 1999. Origins of medial geniculate body projections to physiologically defined zones of rat primary auditory cortex. *Hear Res.* 130:42-61.
- Winograd M, Destexhe A, Sanchez-Vives MV. 2008. Hyperpolarization-activated graded persistent activity in the prefrontal cortex. *Proc Natl Acad Sci USA.* 105:7298-7303.
- Zarrinpar A, Callaway EM. 2006. Local connections to specific types of layer 6 neurons in the rat visual cortex. *J Neurophysiol.* 95:1751-1761.
- Zhang Z-W. 2004. Maturation of layer V pyramidal neurons in the rat prefrontal cortex: intrinsic properties and synaptic function. *J Neurophysiol.* 91:1171-1182.
- Zhang Z-W, Deschenes M. 1997. Intracortical axonal projections of lamina VI cells of the primary somatosensory cortex in the rat: a single-cell labeling study. *J Neurosci.* 17:6365-6379.